Spring 2013

Assembly and characterization of a cell-particle hybrid system as a potential cancer vaccine

Kawther Khalid Ahmed
University of Iowa

ASSEMBLY AND CHARACTERIZATION OF A CELL-PARTICLE HYBRID SYSTEM AS A POTENTIAL CANCER VACCINE

by

Kawther Khalid Ahmed

A thesis submitted in partial fulfillment
of the requirements for the Master of
Science degree in Pharmacy
in the Graduate College of
The University of Iowa

May 2013

Thesis Supervisor: Associate Professor Aliasger K Salem

Graduate College
The University of Iowa
Iowa City, Iowa

CERTIFICATE OF APPROVAL

_____

MASTER'S THESIS

_____

This is to certify that the Master's thesis of

Kawther Khalid Ahmed

has been approved by the Examining Committee
for the thesis requirement for the Master of Science
degree in Pharmacy at the May 2013 graduation.

Thesis Committee: _____
Aliasger K Salem, Thesis Supervisor

_____
Maureen Donovan

_____
Jennifer Fiegel

To the people who made me confident that I could do this; my parents. To the person who enlightened my path throughout this journey; my husband. To those who can always make me smile; my sisters. To the two who bring me joy; my daughters.

ACKNOWLEDGMENTS

I would like to express my gratitude to those who made this thesis possible. First and foremost, I wish to thank my advisor, Dr. Aliasger K Salem for his unlimited support throughout the course of my graduate study. His expertise in the field and knowledgeable guidance were a vital contribution to this work. I would also like to express my deepest gratitude to the Higher Committee of Education Development in Iraq (HCED) for sponsoring me throughout my Master's program and for providing me the opportunity to pursue my graduate study at this institute. My deepest thanks to my thesis committee members Dr. Maureen Donovan and Dr. Jennifer Fiegel for sparing the time and effort to serve on the committee. I would also like to express my appreciation to the postdoctoral fellow in our laboratory, Dr. Sean Geary, for not only his help with animal experiments, flow cytometry, and thesis revision but also for his insights and suggestions that were of tremendous value toward the completion of this work.

This research would not have been possible without the help of all the members of the Salem Lab. Your support and discussions were very helpful and it has been a real pleasure working with you all; Vijaya Joshi, Amaraporn Wongrakpanich (Kae), Sheetal D'mello, Kristan Sorenson, Kareem Ebeid, and our former lab member Dr. Caitlin Lemke.

My appreciation extends to my family and especially my husband Ali. His patience and support made it possible for me to overcome all the challenges associated with my graduate study.

Last but not least, I would like to thank all faculty members, staff members, and graduate students in the division of pharmaceutics and translational therapeutics. They made the graduate study a scientifically rich yet fun-filled experience.

ABSTRACT

Cancer vaccines represent a promising treatment modality for a world-wide health problem. Whether as an adjuvant or as a stand-alone therapy, cancer vaccines represent a tumor-specific and systemic treatment potentially capable of eliminating metastatic lesions without the severe side-effects often associated with chemotherapy. Specifically, whole cell tumor vaccines have shown promise in preclinical and clinical settings and the studies presented here represent the beginnings of an approach to improve the antitumor potency of these vaccines.

This project demonstrates as "proof of concept" the feasibility of manufacturing tumor cell-particle hybrids. The coupled use of these two components, whole tumor cells and cargo-carrying biodegradable particles, as one entity in a cancer vaccine system is a new line of research. Stable cell-particle hybrids were assembled using avidin-biotin chemistry where cargo-carrying PLGA particles (500 nm diameter) were coated with streptavidin and allowed to bind to tumor cells that had been indirectly labeled with biotin (using an integrin-specific biotinylated antibody). That successful cell-particle hybrids were assembled was determined by multiple means, including flow cytometry, laser scanning confocal microscopy and scanning electron microscopy. Two murine tumor cell lines (representing melanoma and prostate cancer) were investigated in this study and successfully demonstrated the general applicability of the assembly method. Particles appeared to be localized on the cell surface (rather than endocytosed) as determined by microscopic imaging. The cell-particle hybrid was shown to be stable to irradiation, an important consideration since whole tumor cells need to be treated with ionizing radiation prior to being used as vaccines in order to render them nonproliferative and immunogenic. We also characterized loading and release profiles of CpG, a prospective vaccine adjuvant, into PLGA particles.

We conclude that we have developed a method for manufacturing cell-particle hybrids comprising PLGA nanoparticles and irradiated tumor cells. The next step would be to use CpG-loaded particles in the assembled hybrid and test the anti-tumor immune efficiency of this cancer vaccine formulation in either a melanoma or prostate cancer model.

TABLE OF CONTENTS

LIST OF TABLES

LIST OF FIGURES

LIST OF ABBREVIATIONS

APCs: Antigen presenting cells

BCG: Bacillus Calmette–Guérin

CpG (-ODN): Cytosine-phosphate-guanine (-oligodeoxyneucleotide)

CTLs: Cytotoxic T-lymphocytes

DCs: Dendritic cells

EDC: 1-ethyl-3-[3-dimethylaminoprpyl] carbodiimide hydrochloride

FDA: Food and Drug Administration

GM-CSF: Granulocyte-macrophage colony-stimulating factor

HMGB1: High mobility group box 1

IFN-γ: Interferon-γ

IgG: Immunoglobulin G

IL: Interleukin

MHC: Major Histocompatability Complex

NHS: N-hydroxysuccinamide

OVA: Ovalbumin

PAMPs: Pathogen associated molecular patterns

PBS: Phosphate buffered saline

PE: Phycoerythrin

PEG: Poly ethylene glycol

PLA: Polylactic acid

PLGA: Polylactic-co-glycolic acid

SEM: Scanning electron microscopy

TAAs: Tumor associated antigens

TSA: Tumor specific antigens

TLR: Toll-like receptor

TNF-α: Tumor necrosis factor-α

CHAPTER I: INTRODUCTION

Cancer is responsible for approximately 25% of deaths in the United States and is a major health concern world-wide. In spite of the declining incidences for some cancer types, others, including melanoma, have been associated with increased incidence rates in both genders [1]. While surgical removal of tumor mass, chemotherapy, and irradiation represent the major treatment interventions, none are tumor specific and they are usually associated with low cure rates [2]. The main challenge in treating cancer stems from the ability of a tumor to metastasize which means that systemic treatment is important. Immunotherapy and cancer vaccines, in particular, can provide a highly tumor-specific treatment that, compared to standard chemotherapy, is generally associated with less severe toxicities [3].

A number of cancer vaccines that have been investigated to tune anti-tumor immunity have shown promising results in preclinical studies for different types of cancers [4-6], and many of these have subsequently reached clinical trials [7-10]. One strategy that has generated particular interest, and is the primary motivation for this project, is the use of GM-CSF-expressing irradiated tumor cells. In fact, vaccines that utilize GM-CSF secreting allogeneic or autologous tumor cells are under development for a range of cancers, including colorectal, breast, pancreatic, and prostate cancer, and are known under the generic name of GVAX ®, many of which have reached clinical trials [11]. However, it is apparent that improvements need to be made to these vaccines in order to increase their therapeutic potency. In the studies reported here we have focused on a method of generating tumor cell-particle hybrids where the particle encapsulates an adjuvant (such as CpG) in order to enhance the cellular cancer vaccine's immunogenic/therapeutic efficacy. This stems from studies recently demonstrating the enhanced therapeutic effect, in a murine tumor model, of combining soluble CpG with a cellular vaccine comprising a GM-CSF-expressing irradiated neuroblastoma cell line [6].

Cancer vaccines: principles

Cancer cells are aberrantly proliferating cells that grow continuously, evading elimination by the host's immune system. The relationship between cancer and the immune system is proving to be a complicated balance of immunosuppressive and immunostimulatory factors that can contribute to the ultimate fate of the tumor. It is generally conceded that tumor cells are often recognized by the immune system at early stages of tumor development. However, effective immune responses are hindered by a process called immunoediting. During this process, tumor cells undergo mutations and phenotypic changes to decrease their immunogenicity and thereby escape tumor immunoeradication [12, 13].

Antigens expressed by tumor cells can be divided into two groups; the first of these are tumor-specific antigens (TSA) that are expressed exclusively by tumor cells, thus representing an ideal target for immunotherapy. TSAs are often mutated products of oncogenes (e.g. RAS) or oncosuppressor genes (e.g. p53) usually arising from point mutations [14]. The second group is tumor-associated antigens (TAA) that are often normal or non-mutated cell proteins expressed mainly by tumor cells and to a limited extent by normal tissues [14]. These include inappropriately expressed developmental proteins normally expressed by fetal tissues [15]. Other examples of TAAs are cancer-testis antigen that arises from activation of silent genes [16]. Cancer vaccines can be developed to target each of these, however, targeting TSA is more problematic because they are linked to highly unique mutations that renders them patient-specific [14] and therefore require individualized vaccine preparation that has been described to be associated with high variability and need for specialized quality control [17]. TAAs can be targeted using whole cell-based vaccines or using individual purified antigen such as proteins, peptides, and polysaccharides delivered by various vector systems often in association with adjuvants [18]. Each type of vaccine is associated with certain advantages and disadvantages, however, there is a strong possibility that targeting a

single antigen will result in limited activation of cytotoxic T lymphocytes (CTLs) that may not provide adequate anti-tumor immunity [16]. On the other hand, whole cell-based vaccines target a broader range of known and unknown antigens leading to activation of correspondingly greater range of CTLs [17].

In general, to stimulate an antigen-specific immune response, the antigen must be taken up by a professional antigen presenting cell known as a dendritic cell (DC). DCs process and present antigen/epitopes on the cell surface in association with major histocompatibility complexes, MHC class I, or MHC class II, proteins. In particular, for an effective anti-tumor CD8+ cytotoxic T lymphocyte immune response to develop, TAAs must be presented by DCs in the context of MHC class I molecules [19]. The primary aim of most cancer vaccines is the activation of tumor-specific CTLs within the patient [20]. Activation of tumor-specific CTLs usually takes place in the draining lymph node (at the site of vaccination) and from there they can travel to, and infiltrate, the tumor microenvironment [20] where they can potentially eradicate tumor cells through a process known as programmed cell death [21].

The ability of the immune system to potentially recognize mutant cell malignancies and limit tumor incidence was recognized in the early 1900s when the hypothesis of immune surveillance was first suggested [22] and, since then, has been supported by abundant findings. These findings include: rejection of transplanted tumors by mice that was shown to be mediated by tumor-specific CTLs [22]; the increase in cancer patients' survival times correlating with increased levels of tumor infiltrating lymphocytes [23]; and a few clinical cases of spontaneous remissions [24]. However, in most cases, the TAA-specific CTLs remain dormant due to active tolerance mechanisms or through anergy [24, 25]. Cancer vaccines targeting TAAs have been shown to stimulate host TAA-specific CTLs [26, 27]. Thus, the major goal of cancer vaccines, in general, is to break tolerance to TAAs and activate otherwise dormant tumor-specific CTLs to an extent capable of eradicating pre-existing tumor and metastases and provide

long term protection, through immune memory, against subsequent tumor recurrence (Figure I.1) [28-30].

Cancer immunotherapy can be subcategorized into either passive immunization, such as the use of antibodies (or adoptive T cell therapy) or active immunization that involves generating an adaptive immune response such as a CTL response in vivo [31, 32]. Examples of active immunizations include: whole tumor cell based vaccines; the use of viruses engineered to express tumor antigens [33]; injection of TSA/TAA with an adjuvant; and the use of TSA/TAA-pulsed DCs as a cancer vaccine [34] of which the recently FDA (Food and Drug Administration)-approved therapeutic prostate cancer vaccine, sipuleucel-T® is an example [35]. Each of these forms of cancer vaccines is being investigated, however, some are associated with major disadvantages such as: 1) inducing a stronger immune response to the vector rather than to the cancer transgene product (TAA), a situation that is often associated with viral vector-based cancer vaccines [36]; 2) vaccines involving purified peptides or proteins offer a limited range of epitopes generally resulting in a less than optimal anti-tumor immune responses [34]; 3) some require costly labor-intensive techniques such as DC-based vaccines [34]. In contrast, whole cell-based cancer vaccines require no vector, have the advantage of exposing the immune system to a wide range of known, and unknown, TAAs [37], and in the case of allogeneic vaccines, they are less labor intensive [17].

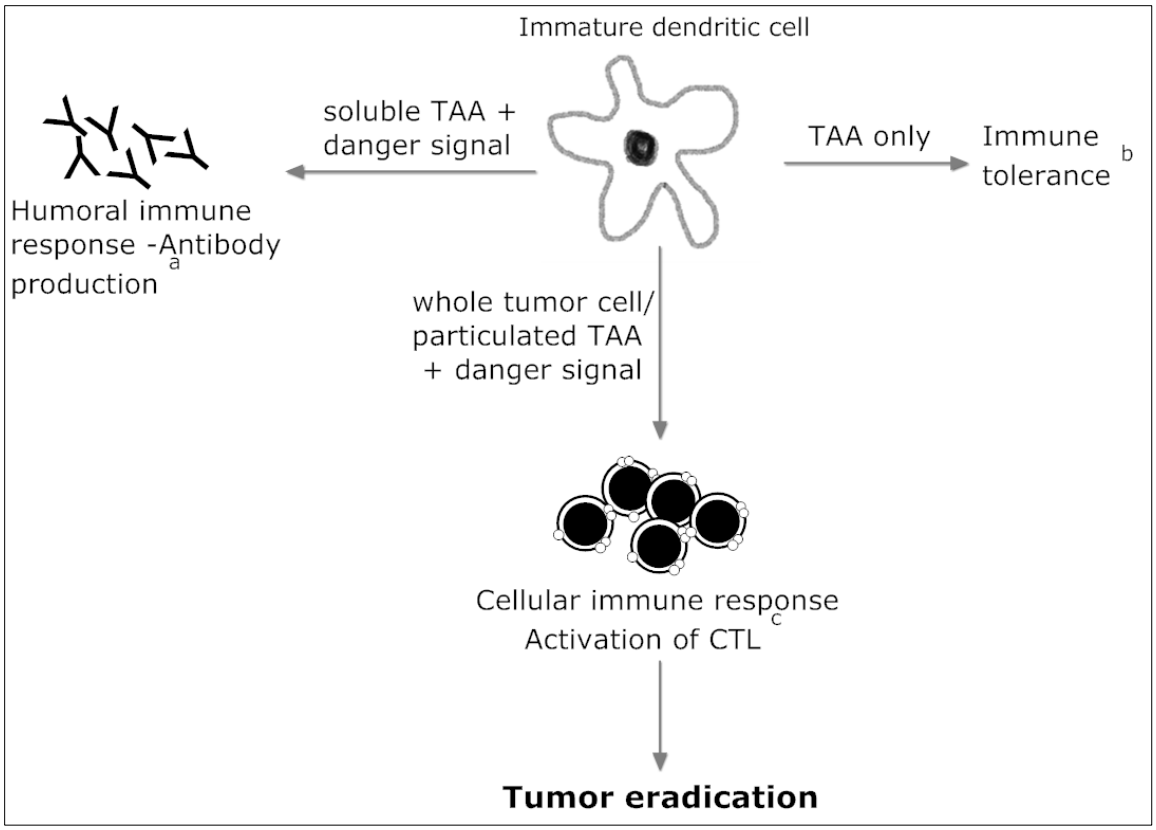

Figure I.1: Immune response pathway depends on vaccine formulation

---

a: Zhang, X.Q., et al., Potent antigen-specific immune responses stimulated by codelivery of CpG ODN and antigens in degradable microparticles. J Immunother, 2007. **30**(5): p. 469-78.

b: Ichim, C.V., Revisiting immunosurveillance and immunostimulation: Implications for cancer immunotherapy. J Transl Med, 2005. **3**(1): p. 8

c: Chiang, C.L., F. Benencia, and G. Coukos, Whole tumor antigen vaccines. Semin Immunol, 2010. **22**(3): p. 132-43.

Particles in cancer vaccines

Polymeric particles in drug delivery have a broad range of applications that include preventive, diagnostic, and therapeutic medical applications [38, 39]. Polymeric particles can, depending on the formulation, offer a variety of advantages over conventional soluble drug administration. Two examples are: 1) tissue-specific targeting with surface engineered particles; and 2) forming a depot that ensures long-lasting release of the loaded active pharmaceutical ingredient [40].

Particle-based cancer vaccines represent a promising anti-tumor strategy for a number of reasons [41]. These include: 1) protection of the encapsulated payload from premature degradation [42]; 2) co-delivery of encapsulated materials (e.g. TAA and adjuvants) to the same DC; 3) certain particles themselves can serve as immune adjuvants [43]. These vaccines are being studied for the prevention and treatment of a wide variety of diseases where the immune system can play a significant role. These include, but are not limited to, cancer [44], leishmania [45], anthrax [46], hepatitis [47], and even allergies [48].

Many studies have investigated vaccination with particulated vaccines that co-deliver to DCs the antigen and the adjuvant versus vaccination with independently particulated or soluble forms of either one. Results have shown that co-delivery of adjuvant and antigen to DCs triggers stronger immune responses (as measured by IgG_{2a} responses) compared to soluble forms of both and to soluble adjuvant co-administered with particulated antigen [30]. Another study compared the immune response elicited by a soluble molecular fusion product comprising ovalbumin (OVA) as antigen and CpG as the adjuvant versus the immune response triggered by microparticles encapsulating both [49]. Both formulations elicited strong immune responses (as measured by IgG_{2a} and INF-γ responses), however, particulated vaccines elicited stronger immune responses than the soluble molecular fusion product. The study hypothesized that the particulated formulation may have been acting as a depot thereby providing sustained antigen

presentation to DCs. Another possibility is that the particulated material was protected from premature degradation by nucleases and proteases.

Among the variety of materials investigated for particulated drug delivery and cancer vaccines, polylactic-co-glycolic acid (PLGA) polymer is the most studied and represents an excellent candidate for vaccine delivery. PLGA has been FDA approved and is biodegradable with safe degradation end products [50, 51] (Figure I.2). PLGA is a polyester polymer composed of lactic acid and glycolic acid units in variable ratios. The ratio of the two components affects the degradation rate of the formulated particles and the release profile of their cargo [41, 52].

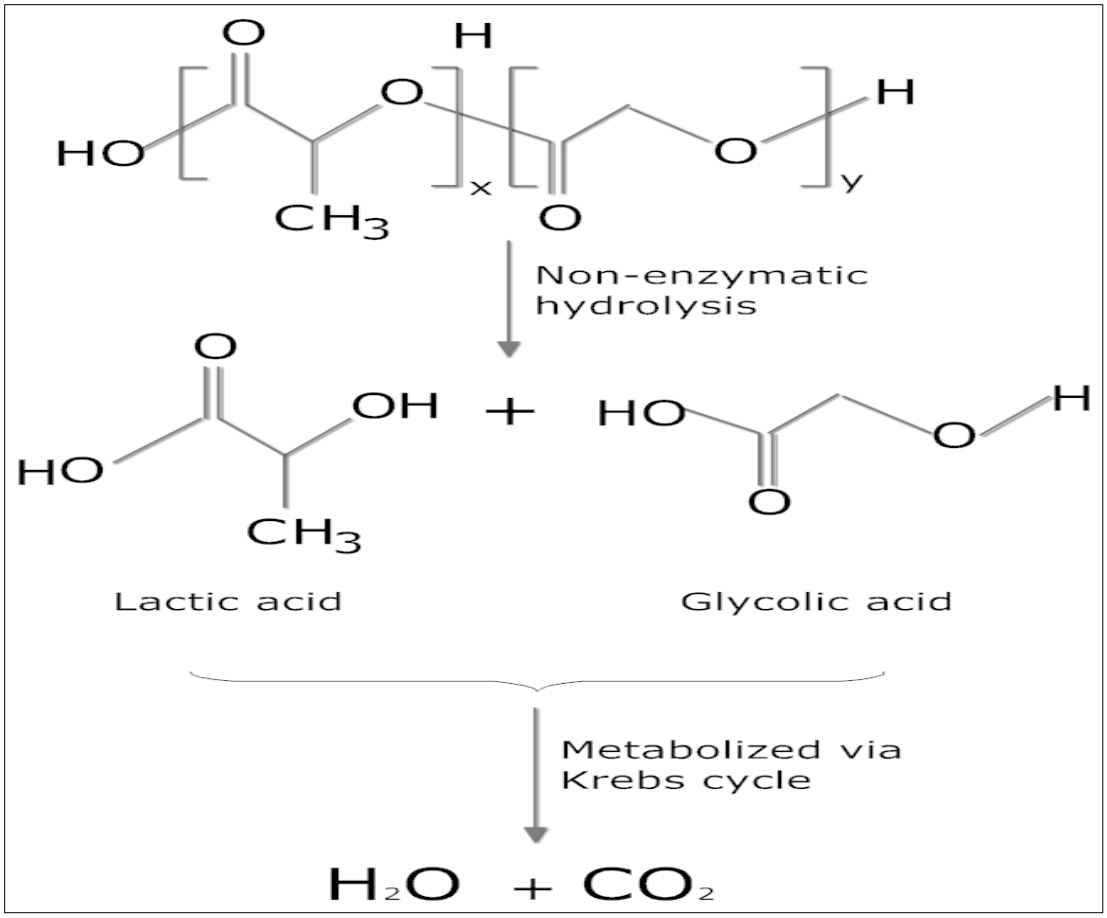

Figure I.2: Structure of the PLGA polymer and its biodegradation pathway

An important consideration in formulating particles as vaccines is their size. Particle size has been reported to affect the type and extent of the immune response triggered by the particulated vaccine [53-55]. For a particle-based vaccine system to be effective, the particles should be taken up by DCs. Ideally the loaded antigen will then be cross-presented and a CTL-based immune response will be initiated. This requires particle sizes small enough (less than 10 µm) to be efficiently engulfed by DCs, yet sufficiently large to avoid non-specific uptake by non-APCs (antigen presenting cells) [56]. It has been reported that particles larger than 500 nm will result in humoral immune responses [43]. Other studies have shown preferential uptake of 300 nm PLGA particles over 1 and 7 µm particles by DCs in vitro [53]. For the purposes of this project, particle size per se is less relevant since we are concerned with cell-particle hybrids. Thus, primary considerations are that the size of the particle complex does not exceed 10 µm and that the particle size does not negatively affect the stability of the hybrid complex. Although there are few data available in this respect, one study has shown that particles in the range of 200-500 nm achieve more stable binding to red blood cells than larger (800 nm) or smaller ones (100 nm) after exposure to sheer forces [57].

In spite of the advantages offered by particles as vaccine vectors, they generally employ one or very few tumor antigen(s). This limits the immune response and results in activating only a small pool of TAA-specific CTLs, possibly leading to a clinically inefficient anti-tumor immune response [16]. Hence, there is a need for a vaccine vector capable of delivering a wide array of tumor antigens and simultaneously co-delivering the adjuvant to the same DCs. The cell-particle hybrid vaccine has the potential to achieve this.

Irradiated tumor cells as cancer vaccines

An essential component of cancer vaccines is the tumor antigen against which the immune response is to be induced. Tumor antigens can be introduced into vaccine vectors

as purified antigen or DNA encoding the tumor antigen, or as whole tumor cell lysate. Alternatively, the whole intact tumor cell can be used as the cancer vaccine. As already stated, the use of whole tumor cells as vaccines ensures delivering an array of tumor antigens rather than just one tumor antigen, therefore increasing the potential for activating many tumor-specific CTL clones [6]. However, it is essential that the tumor cells used as the vaccine are rendered both immunogenic as well as being incapable of proliferating at the time of vaccination [3, 58]. These two properties can be achieved by treating the cell with a lethal dose of ionizing radiation prior to vaccination.

Cell death can take one of two pathways, necrosis or apoptosis [59]. Necrosis is characterized by cell membrane rupture and release of the intracellular components and can be induced in vitro by repeated freeze-thaw cycles. On the other hand, apoptosis or programmed cell death is a slower process and can be induced both in vitro and in situ by ionizing irradiation or certain cytotoxic drugs [60]. For cancer vaccine formulations necrosis is induced to produce cell lysate-based vaccines while apoptosis is triggered when the whole tumor cell is used as a cancer vaccine [15]. However, the immune response triggered in each case is substantially different. With necrosis, a raw mixture of all cellular components that contains soluble tumor-derived proteins is released. These soluble antigens can be taken up by DCs via micropinocytosis and loaded onto MHC class II molecules [15]. This pathway was shown to lead to low antigen cross-presentation and therefore low or no stimulation of CTLs [61, 62]. The term cross-presentation refers to the process of exogenous antigen being taken up by DCs and its ultimate expression in association with MHC class I on the DC surface, an event that favors stimulation of CD8+ T lymphocytes/CTLs [63]. Besides a lack of CTL activation, another problem associated with necrotic cell death is the release of abundant amounts of heat shock proteins [15, 62] that could, depending on their type, lead to induction of immune tolerance[64]. On the other hand, apoptosis can be immunostimulatory depending on the stimuli [60]. For cancer vaccine purposes it is highly desirable that

apoptotic cell death be immunogenic [65]. In fact, only recently has the distinction between immunogenic and non-immunogenic apoptotic cell death been defined. Researchers have shown that for an apoptotic tumor cell to be capable of inducing an immune reaction, translocation of calreticulin, a calcium binding protein, from the endoplasmic reticulum of tumor cells to the cell surface is a key requirement [65, 66]. This event occurs early in apoptosis [60] when cell death has been induced by γ-irradiation or certain chemotherapeutic agents [67] (Figure I.3). The translocation of calreticulin to the cell surface of the dying tumor cell promotes its phagocytosis by DCs [15, 60, 68]. Another potentially important component of immunogenic cell death is the release of high mobility group box 1 (HMGB1). This molecule was suggested to act as an endogenous adjuvant that stimulates the innate immune system [69]. It has been shown, in clinical settings, that HMGB1 is released from lethally irradiated cells and the tumor specific CTL-response was correlated to serum levels of HMGB1 [70]. It has also been suggested that HMGB1 has a role in enhancing antigen cross-presentation. When HMGB1 binds a surface receptor on DCs it can inhibit the fusion of the phagosome with lysosomes, thus preventing antigen/epitope degradation. [15]

It has been suggested that immunization with whole cell vaccines generates stronger T-cell responses [71] and higher delayed-type hypersensitivity reactions [72] than immunization with tumor lysates derived from the same cells. The underlying mechanism is not well characterized but it is believed that the presence of immunosuppressive molecules in tumor lysates may promote immune tolerance [15]. Another suggested mechanism is that an intact cell membrane is required for: 1) calreticulin expression [66]; and 2) sequestering cytoplasmic components that may inhibit the immune response within the cell [66].

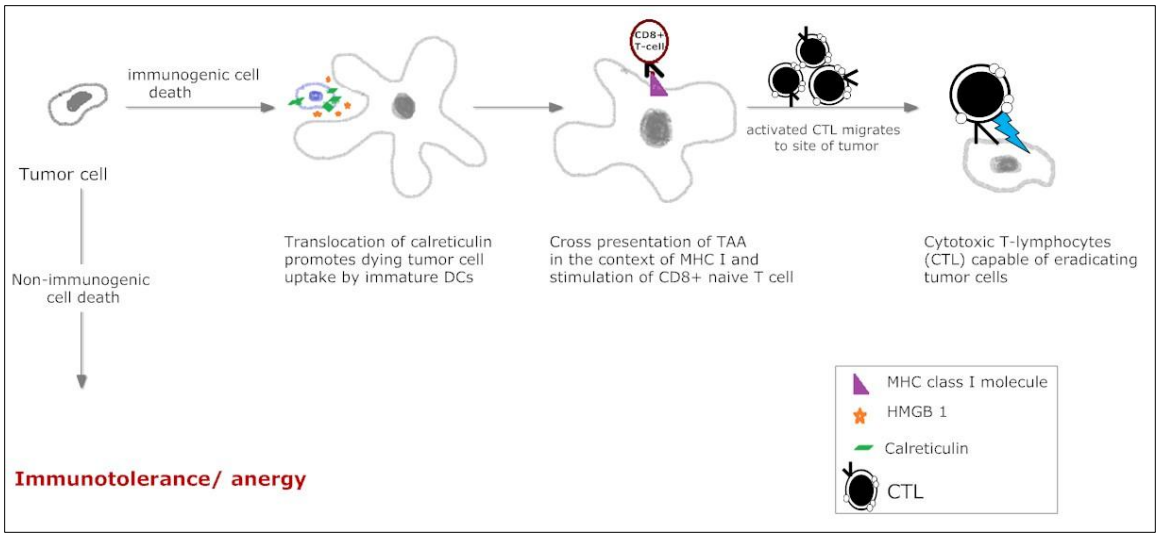

Figure I.3: Immunogenic apoptotic cell death

An important element in cancer vaccines is the appropriate stimulation of DC maturation such that efficient cross-presentation of the introduced antigen occurs. At least five types of receptors are expressed by DCs that are reported to be responsible for driving DC maturation [19]. These include Toll-like receptors (TLRs) and cytokine receptors that are important in cancer vaccines. Others are tumor necrosis factor receptors, Fc receptors for antibody binding, and cell death sensors. DC-driven maturation via each receptor family leads to phenotypically distinct DC populations that will, in turn, result in distinct types of immune responses [19]. Thus, to achieve the desired activation of tumor-specific CTLs, it is desirable to incorporate (into the vaccine formulation) immunomodulators capable of stimulating appropriate DC maturation. To elaborate, it has been demonstrated that irradiated B-cell lymphoma tumor cells alone are incapable of enhancing survival rates of experimental animals whereas the therapeutic vaccination with irradiated tumor cells transfected with genes encoding for co-stimulatory molecules enhances their immunogenicity and anti-tumor effectiveness [5]. A

co-stimulatory molecule that has generated particular interest is granulocyte-macrophage colony-stimulating factor (GM-CSF).

GM-CSF is a pleiotropic cytokine that is capable of triggering DC chemotaxis and maturation [3, 73]. A significant study compared the effectiveness of different cytokines including IL-2, IL-4, γ-IFN, TNF-α, and GM-CSF in boosting the protective and therapeutic efficiency of irradiated tumor cell vaccines [58]. The study demonstrated that irradiated murine melanoma B16.F10 cells alone did not lead to anti-tumor immunity whereas irradiated cells expressing GM-CSF were capable of eliciting strong anti-tumor immunity resulting in rejection of pre-established tumors and increased survival of tumor challenged mice. Compared to the other cytokines tested, GM-CSF had a superior role in modulating vaccine efficacy such that more potent anti-tumor responses were elicited. Furthermore, the immune response was long lasting such that mice vaccinated with GM-CSF expressing cells could resist live tumor cell challenge several months later, a result that was not observed with animals vaccinated with irradiated cells expressing other cytokines.

Several other studies have compared the effect of vaccination using irradiated tumor cells expressing GM-CSF in a range of tumor models. In a murine melanoma tumor model, vaccination with irradiated GM-CSF-modified tumor cells resulted in stronger systemic anti-tumor immunity compared to non-GM-CSF-modified irradiated tumor cells [74]. Similar findings were found in a phase I clinical trial with metastatic non-small-cell lung carcinoma where vaccination with autologous tumor cells, transduced to secrete GM-CSF, succeeded in prolonging survival for some patients [10]. These results suggest the importance of incorporating GM-CSF into whole cell-based cancer vaccines to improve vaccine efficiency.

Role of CpG in modulating the effectiveness of cancer vaccines

Pathogen-associated molecular patterns (PAMPs) can bind to Toll-like receptors (TLRs) expressed by DCs and trigger their maturation, which in turn can lead to the activation of CTLs [19, 75]. These PAMPs, or "danger signals", are pathogen-derived components such as bacterial wall products, DNA sequences, and lipids [76]. The fact that some PAMPs can activate DCs to preferentially stimulate CTL responses has further encouraged their incorporation as adjuvants into cancer vaccines. The use of PAMPs in cancer vaccines can be dated back to more than 30 years ago, prior to the discovery of TLRs, where irradiated hepatocellular carcinoma cells admixed with attenuated live bovine tuberculosis, bacillus Calmette–Guérin (BCG), were examined for a potential immunotherapeutic effect against established micrometastases in guinea pigs [77]. The study demonstrated that incorporating BCG into the vaccine greatly enhanced the survival rate of tumor-challenged animals. However, being a whole bacterium, BCG is usually associated with strong inflammation [78] and it has not been given FDA approval. Meanwhile, the only FDA approved adjuvant for use in cancer vaccines, alum, is inferior to PAMPs at generating CTL responses [79]. More recently, a bacterially-derived DNA sequence containing unmethylated cytosine phosphate guanine (CpG) oligodeoxyneucleotide (ODN) motifs was found to increase immunostimulatory potency of cancer vaccines [78, 80, 81]. Unmethylated CpG sequences are rare in the mammalian genome, thus it is hypothesized that the presence of unmethylated CpG is sensed by the mammalian innate immune system as a "danger signal", flagging the possible presence of a bacterial infection [42]. CpG binds specifically to TLR-9 receptors expressed by DCs and results in their subsequent maturation into immunostimulatory cells capable of

preferentially activating CTLs over B-lymphocytes [82]. The effectiveness of CpG in polarizing immune responses toward CTL stimulation and improving cancer vaccine efficiency has been established for different cancer models such as lymphoma [83] and neuroblastoma [6]. Several strategies have been implemented to investigate possible delivery options of CpG as an adjuvant in cancer vaccines and have been extensively reviewed [78]. Examples of such are the use of biodegradable microparticles co-encapsulating CpG and the tumor antigen versus microparticles encapsulating each alone [30] where the advantageous contribution of CpG was demonstrated by elevated IgG_{2a}/IgG_1 which is considered indicative of inducing cellular immune responses. Other techniques involve liposomes and multicomponent nanorods. To elaborate, CpG was co-encapsulated with OVA as a model tumor antigen in liposomes and used to immunize mice intravenously, then the tumor-specific immune response was measured [84]. The liposomal combination of OVA and CpG showed improved activation of antigen-specific CTLs over liposomal encapsulation of the antigen alone. In a separate study, gold-nickel nanorods were formulated by electrodeposition and covered by OVA antigen and DNA-encoding for CpG motifs. These nanorods were used to vaccinate mice in the abdominal region using a gene gun where they generated antigen-specific humoral and cellular immune responses [85].

An important study recently investigated the role of CpG in cancer vaccines involving whole tumor cells has demonstrated the importance of co-delivery of CpG and the tumor cell to the same DC [86]. In this study CpG was covalently linked to apoptotic E.G7 cells and used to vaccinate mice prophylactically, therapeutically and post tumor resection. The prophylactic and therapeutic efficiency of the vaccine was examined

against several controls including apoptotic cells admixed with but not covalently bound to CpG. Vaccination with CpG-linked apoptotic tumor cells resulted in remarkably enhanced protection against tumor challenge and metastasis as well as significantly slowing pre-established tumor growth compared to other vaccination formulations tested. This direct coupling of CpG was suggested to confine CpG to the vaccination area and result in enhanced vaccine performance. These results agree with another study demonstrating the crucial role of co-localization of CpG and tumor antigen in DCs for efficient activation of tumor specific CTLs [87]. These findings highlight the need for a cancer vaccine that delivers CpG, tumor cells, and any other adjuvant (such as GM-CSF) to the same DC for efficient anti-tumor immunity.

As different danger signals will trigger immune responses via different pathways, combining those stimulatory molecules may have synergistic effects. Consequently, researchers are investigating different combinations depending on the desired immune response [88]. A particularly relevant combination that showed enhanced tumor-specific CTL activation in an irradiated tumor cell-based vaccine was CpG and GM-CSF. Two important studies have been conducted in this regard. First, a vaccine composed of CpG, GM-CSF, and tumor antigen (all soluble) was used in a murine B-cell lymphoma model. The vaccine resulted in an increased production of antigen-specific antibodies and increased survival of mice compared to formulations involving either CpG or GM-CSF alone [89]. The second study involved a therapeutic vaccine composed of soluble CpG admixed with irradiated GM-CSF-secreting tumor cells in a murine neuroblastoma model [6]. In this study, mice inoculated with wild type tumor cells were vaccinated with the above formulation three days post inoculation. The vaccine generated tumor-specific CTLs capable of eradicating established small tumors and generated systemic tumor-specific immunity where vaccinated mice rejected tumor rechallenges. In contrast, other

vaccine formulations tested in this study (irradiated GM-CSF secreting cells alone and non-irradiated GM-CSF secreting cells plus CpG) failed to prevent tumor growth. This latter finding emphasizes the significance of incorporating CpG as an adjuvant in cancer vaccine formulations involving GM-CSF secreting tumor cells and the need to irradiate cells prior to vaccination.

As discussed earlier, the use of whole tumor cells as a cancer vaccine and the contribution of CpG and GM-CSF to cancer vaccine effectiveness were originally confirmed separately. Recent demonstrations of the enhanced effect of their combination in curing established tumors and providing long term protection against subsequent tumor challenges does indeed highlight the potential of this formulation in achieving the ultimate goal of cancer vaccines as a curative and protective treatment modality. These findings and those related to CpG and antigen co-localization in DCs were the motive for designing a cancer vaccine system that involves irradiated GM-CSF secreting tumor cells physically linked to particulated CpG in the form of a cell-particle hybrid where we hypothesize that the attachment of particles to cells ensures their co-delivery to the same DC and leads to enhanced anti-tumor immunity.

Cell-particle hybrids as potential vaccines

Many studies have looked at cell-particle interactions in terms of their effects on cellular viability, particle uptake by cells, and specific cell targeting of modified particles [50, 90, 91]. However, assembling a cell-particle hybrid as a vaccine delivery vehicle represents a new area of research. Assembly of cell-particle hybrid systems have been seldom reported to date and none were specifically designed as cancer vaccines. The first reported cell-particle hybrid, to our knowledge, was an erythrocyte-particle hybrid designed for sustained drug delivery. This system involved attaching polystyrene particles of different sizes to erythrocytes via non-specific adhesion followed by surface modification of the assembled erythrocyte-particle complex with polyethylene glycol

(PEG). The authors suggested that particles could be loaded with the drug of interest and thereby the assembly could increase loaded particles circulatory half-life enabling longer systemic release of their cargo [57]. Another cell-particle hybrid designed for targeted cancer chemotherapy involved anchoring neutravidin-coated polystyrene 40 nm nanoparticles onto biotinylated mesenchymal stem cells [92]. Another cell-particle conjugate involved surface conjugation of synthetic particles (liposomes (217 nm), multilameller lipid particles (320 nm), and lipid coated PLGA particles (230 nm) onto hematopoietic stem cells and T cells via attaching functionalized particles to thiol residues on the cell surface [93]. The particles were loaded with adjuvant drug (cytokines or glycogen synthase kinase-3β inhibitor) for pseudo-autocrine stimulation of the conjugated cells. Finally, a cell-particle hybrid was developed previously in our laboratory, involved conjugating poly (lactic acid)-poly (ethylene glycol) (PLA-PEG) microparticles to tumor cells using avidin-biotin linkages [94]. Results showed cell-particle binding to some extent, however, the level of particle binding needed to be higher for practical vaccine applications. While those studies demonstrate the basic feasibility of the cell-particle hybrid concept, we aim to take this concept further by assembling an optimized cell-particle conjugate that is specifically designed for vaccination purposes.

Project overview, hypothesis, and specific aims

Cancer represents a challenging health problem and current interventions are not adequate. In addition, most standard systemic therapies are associated with high rates of toxicity [2]. Cancer vaccines represent a treatment modality that not only aims at specifically eradicating the existing tumor but also at providing long-term protection against tumor recurrence and metastasis. While the application of cancer vaccines has had sporadic attention from clinicians over the past century, major advances in our understanding of the relationship between the immune system and tumor cells over the last 20 years have strongly validated the application of cancer vaccines as potential

therapies for a range of cancer types [15, 63, 95, 96]. The use of irradiated GM-CSF-secreting tumor cells and the use of polymeric particles as cancer vaccines have been extensively studied [30, 44, 58] and some have reached clinical trials [10]. However, the assembly of a cell-particle hybrids designed for cancer vaccination purposes, to our knowledge, is an unexplored area.

While demonstrating the advantageous combining of CpG to vaccines involving GM-CSF-secreting tumor cells was achieved using soluble CpG, studies have later demonstrated that CpG covalently linked to tumor cells is more effective [86]. Here we aimed to assemble a cell-particle hybrid vaccine system where the CpG-loaded particles will not only serve to confine CpG to cells, as described earlier, but also add a level of flexibility to the system, thereby allowing alternatives, or additions, to CpG to be used.

The first step toward the suggested vaccine system is efficiently assembling cell-particle hybrids. In this project, we hypothesize that using established avidin-biotin chemistry, stable cell-particle hybrids can be assembled with the potential for use as a cancer vaccine.

The ultimate goal of the project is to achieve a cell-particle hybrid by conjugating CpG-loaded PLGA particles to irradiated GM-CSF-secreting tumor cells. As a "proof of concept" of the ability to conjugate particles to cells in an efficient manner, we plan to develop a cell-particle assembly using PLGA particles loaded with rhodamine and non-GM-CSF secreting cells as there would be no need to use CpG-loaded particles for these initial optimization experiments and GM-CSF secretion should not interfere with the proposed method of binding. Once a stable cell-particle hybrid is achieved with the blank particles and non-modified cells, we can then use CpG-loaded particles and GM-CSF secreting cells to assemble the cell-particle hybrid that would be tested for cancer vaccine applications (Figure I.4).

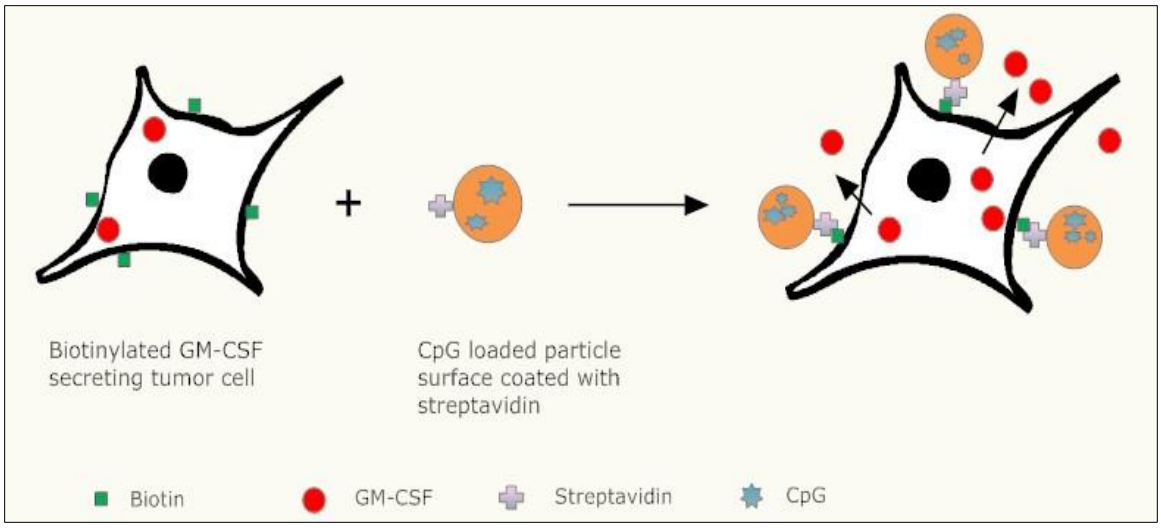

Figure I.4: Schematic of the cell-particle hybrid suggested in this project

To test our hypothesis we will attempt to achieve the following aims:

1. To create stable cell-particle hybrids incorporating either the murine melanoma cell line, B16.F10, or the murine prostate cancer cell line, RM11. This will involve two key steps:

(a) Fabricating and surface functionalizing rhodamine-labeled PLGA particles.

(b) Surface-modifying tumor cells with biotin.

2. To establish the minimum dose of lethal irradiation required to render tumor cells (within the cell-particle hybrid) non-tumorigenic.

CHAPTER II: MATERIALS AND METHODS

Fabrication of PLGA particles

Particle preparation and characterization

Blank PLGA particles were prepared by double emulsion (w/o/w) solvent evaporation method (Figure II.1). In short, 75 µl 1% PVA (Polyvinylalcohol, Mowiel®,Sigma Aldrich , St Louis MO) representing internal water phase (W1) was emulsified into 200 mg PLGA 75:25 initiated with glycolic acid (molecular weight 68.1 kDa, 0.59 dl/g inherent viscosity, Lactel absorbable polymers, Pelham AL) in 2 ml DCM (Dichloromethyl methane, Sigma Aldrich, St Louis MO) polymer solution using a sonic dismembrator (Model FB 120 equipped with an ultrasonic converter probe; Fisher Scientific, Pittsburgh, PA) at 40% amplitude for 30 seconds. This primary emulsion was emulsified into 8 ml 2.5% PVA solution, W2, using previous sonic conditions to form the secondary emulsion. The secondary emulsion was then poured into 30 ml 1% PVA solution. DCM was allowed to evaporate from the secondary emulsion by stirring the emulsion in a fume hood for 1.5 hour on magnetic stirrer (Coring Stirrer/ Hot Plate, model PC-420). Submicron sized particles were then collected by differential centrifugation modified from the method described by Joshi *et al.* [53]. For this project original particle suspensions were centrifuged at 4000 rpm (2888 ×g) for 5 minutes (Eppendorf centrifuge 5804 R, Eppendorf, Westbury, NY). Submicron sized particles were then collected from the supernatant by spinning at 8500 rpm (10000 ×g) for 10 minutes (AccuSpin™ 400 Fisher Scientific, Germany). Collected particles were washed twice with distilled water and lyophilized overnight (FreeZone 4.5, Labconco Corporation, Kansas city, MO). When fluorescent particles were needed, 2 mg rhodamine B (Sigma, St Louis, MO) were added to the polymer solution. CpG-loaded PLGA particles were prepared using 3 mg CpG ODN 1826 (type B sequence 5'-TCCAGACGTTCCTGACGTT-3', Integrated DNA Technologies, Coralville, IA) in 75

µl 1% PVA (Polyvinylalcohol, Mowiel®,Sigma Aldrich , St Louis MO) as the internal aqueous phase, W1.

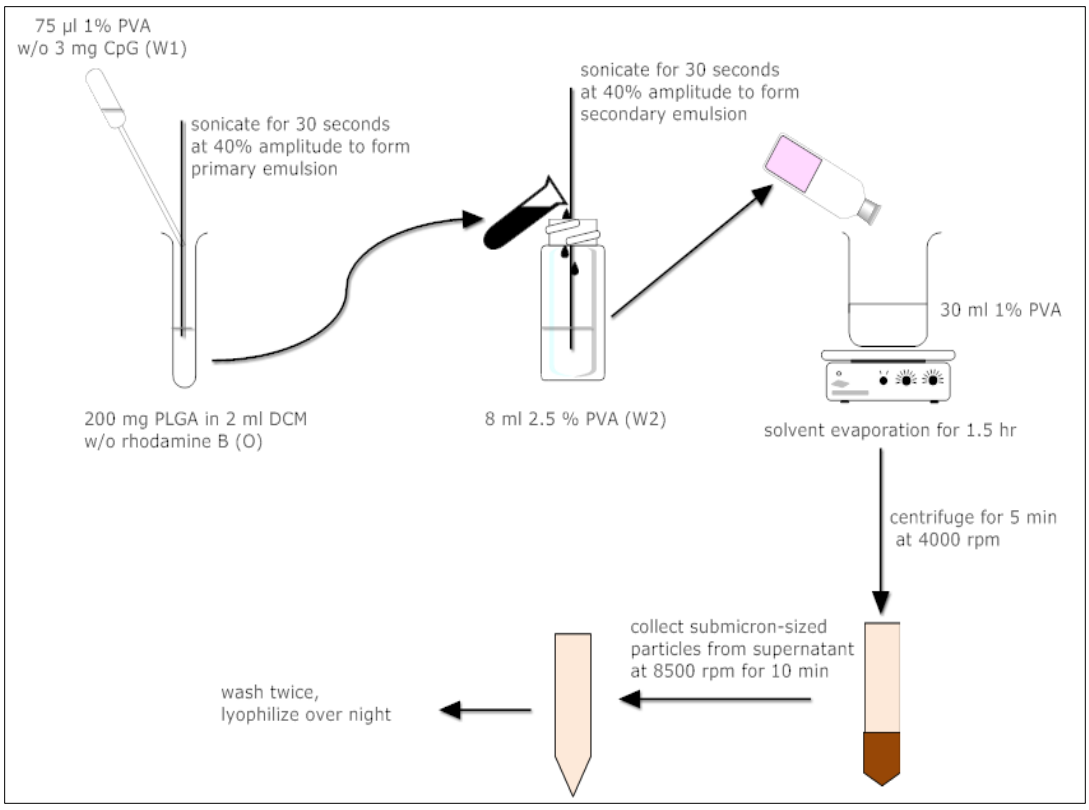

Figure II.1: Schematic presentation of double emulsion solvent evaporation method

Percent recovery of submicron sized particles from total fabricated particles was calculated as follows:

Equation II.1:

$$\text{Percent recovered} = \frac{\text{weight of particles retrieved in the 2nd centrifugation}}{\text{weight of particles retrieved in first centrifugation} + \text{weight of particles retrieved in 2nd centrifugation}} \times 100$$

Prepared particles were characterized for shape, surface morphology, size, and zeta potential. The shape and surface morphology of the particles were examined using scanning electron microscopy imaging (SEM). Lyophilized particles were spread on a silicon wafer attached to an aluminum stub. Particles were then coated with gold-palladium for 3 minutes using Argon beam K550 sputter coater (Emitech Ltd, Kent, England) prior to imaging via SEM, (Hitachi S-4800 SEM, Hitachi High Technologies, Ontario, Canada) at 2 kV accelerating voltage. The size of blank and CpG-loaded particles was measured from a suspension of 1 mg particles in DI water using a Zetasizer (Nano-ZS, Malvern, UK) at 173° back scatter detection angle. For rhodamine-loaded particles, size was measured from SEM images and analyzed using ImageJ software (US National Institutes of Health, Maryland) with n = 100. This method of particle sizing was validated by analyzing SEM images of blank and CpG-loaded particles with ImageJ and the results were compared to the Zetasizer readings. Zeta-potential was measured using the Zetasizer (Zetasizer, nano series. Nano-ZS, Malvern, UK), n=3.

CpG loading and release profile

To estimate total CpG loaded and loading efficiency, 5 mg of CpG-loaded particles were incubated with 0.3 N NaOH on a rotary shaker (Drummond Scientific Co, Broomall, PA) until all the polymer was dissolved. The clear solution was neutralized with 1 N HCl. CpG concentration was then estimated using fluorescence OliGreen® kit (Molecular Probes, Eugene, OR) with excitation and emission wavelengths of 480 nm and 520 nm, respectively. Fluorescence intensity was measured on SpectraMax® M5 multimode microplate reader (Molecular Devices, Sunnyvale, CA).

Total loading and loading efficiency were calculated as follows:

Equation II.2:

$$\text{Total loading} = \frac{\text{CpG concentration in neutralized solution} \times \text{neutralized solution volume}}{\text{weight of degraded particles}}$$

Equation II.3:

$$\text{Loading efficiency} = \frac{\left(\begin{matrix}\text{weight of PLGA polymer used in} \\ \text{particle fabrication}\end{matrix} \times \text{total loading}\right)}{\text{amount CpG used}} \times 100$$

To examine the in vitro release profiles of CpG from PLGA particles, 25 mg of particles were suspended in 700 µl phosphate buffer saline (PBS) at pH 7.4 and incubated at 37°C using an incubator shaker operated at 200 rpm/min. Samples were collected at predetermined time points by centrifugation at 8500 rpm (10000 ×g) (AccuSpin™ 400 Fisher Scientific, Germany) for 10 minutes and fresh PBS was supplied to maintain sink conditions. Quantification of released CpG was also performed using an OliGreen® kit.

Surface saturation of fabricated PLGA particles with streptavidin

Streptavidin was surface conjugated on PLGA particles using EDC/NHS chemistry. Particles were suspended in 0.1 M MES buffer pH 5.1 (MES, 2-(N-Morphino) ethanesulfonic acid, Sigma Aldrich, St Louis MO). EDC (1-ethyl-3-[3-dimethylaminoprpyl] carbodiimide hydrochloride, Thermo Scientific, Pierce Biotechnology, Rockford IL) solution in MES buffer was added at a ratio of 1 mg EDC: 1 mg particles (~370 molar excess) and incubated for 2 minutes on a magnetic stirrer operated at speed level 6. Then, sulfo-NHS (N-hydroxysulfosuccinamide, Thermo Scientific, Pierce Biotechnology, Rockford IL) in MES buffer was added at a ratio of 1.23 mg sulfo-NHS:1 mg particles (~370 molar excess). EDC and sulfo-NHS excess were empirically determined. Activation continued with stirring at same stirring speed for 2 hours according to product instructions. Activated particles were recovered by centrifugation at 8500 rpm (10000 ×g) (AccuSpin™ 400 Fisher Scientific, Germany) for 10 minutes and washed twice in PBS. To detect the basic ability to bind streptavidin to particle surfaces using EDC/NHS chemistry, we incubated 1 mg of EDC/NHS-treated

particles (in 100µl PBS suspension) with fluorescently labeled streptavidin, streptavidin-PE, (eBioscience) at a starting ratio of 0.06 µg/ mg particles according to product instructions and incubated for 30 minutes in the dark at room temperature. Particles were washed three times with PBS to remove unbound streptavidin-PE. As a control, non-EDC/NHS treated particles and EDC/NHS treated particles blocked with 1% bovine serum albumin (BSA) (Albumin, Bovine, Sigma Aldrich, St Louis, MO) were also incubated with streptavidin-PE in parallel. Conjugation of streptavidin was detected by measuring PE fluorescence using flow cytometry (FACSan™, Becton, Dickinson) and data was analyzed using FlowJo analysis software (Tree Star, Stanford).

To optimize the amount of streptavidin required to saturate the particle surface, we ran a pilot study of n=1 where we incubated EDC/NHS treated particles with increasing amounts of streptavidin-PE/mg particles at the range of 0.06 – 8 µg streptavidin-PE/mg particles and increased surface conjugation was determined by increased PE fluorescence signal.

To ensure the availability of conjugated streptavidin for biotin binding, we incubated EDC/NHS treated particles with unlabeled streptavidin (Prospec protein specialist Ness Ziona, Israel) at the final optimized ratio. Those streptavidin-coated PLGA particles were then incubated with fluorescein biotin at a final concentration of 20 µg/ml for 30 minutes (Thermo Scientific, Pierce Biotechnology, Rockford IL). As a control, activated particles that were not streptavidin-coated were incubated with biotin fluorescein in parallel. Binding was detected using flow cytometry where relative fluorescein fluorescence was measured.

Since the process of particle surface saturation with streptavidin involves incubation of the particles in aqueous media, we looked at expected CpG loss during the surface modification process. In a pilot study (n = 1), CpG-loaded particles were coated with unlabeled streptavidin as described earlier. Streptavidin-modified CpG-loaded particles (5 mg) were degraded in 0.3 N NaOH until all the polymer was dissolved. The

solution was then neutralized with 1 N HCl and the remaining CpG was estimated using fluorescence OliGreen® kit. Percent CpG loss was calculated from the following equation:

Equation II.4

$$\text{Percent CpG lost} = [1 - \frac{\text{remaining CpG}}{\text{initial loading}}] \times 100$$

To investigate the ability of streptavidin surface-modified CpG-loaded particles to release the remaining CpG, a release study was performed analogous to that previously described (page 23) using 10 mg streptavidin-coated CpG-loaded particles.

Cell surface modification

Murine melanoma B16.F10 cells (ATCC- CRL 6475™, Manassas VA) were maintained in DMEM 1X complete media (Dulbecco's Modified Eagle's medium, Gibco/ Life Technology, Grand Island, NY) supplemented with 10% fetal bovine serum (Atlanta Biological, Lawrenceville, GA), HEPES buffer, 1M ((4-(2-hydroxyethyl)-1-piperazineethanesulfonic acid), sodium pyruvate (100 mM), Glutamax™ (100X), 1% each (all were purchased from Gibco/ Life Technology, Grand Island, NY), and 0.5 % gentamicin sulfate (50 mg/ml) (Biowhittaker® Lonza, Walkersville, MD). Cells were incubated in a 5% CO_2 cell culture incubator at 37°C (Sanyo, model MCO-20AIC by Sanyo Electric Biomedical Co, Ltd, Japan). Cells were biotinylated using anti-mouse/rat CD29 (Integrin β1) biotin (eBioscience). Adequate expression of β1integrin on the cell surface was determined by immunofluorescence assay. Cells were trypsinized (0.25% Trypsin-EDTA 1X, Gibco by Life Technology, Grand Island, NY), washed twice with media and suspended in ice-cold media at a concentration of 2×10^6 cell/ml, anti-mouse/rat CD29 (Integrin β1) biotin was added to a final concentration of 5 µg/ml. Cells were incubated for 25 minutes on ice. Excess antibody was removed by washing twice using ice-cold media. Streptavidin-PE was added at a final concentration of 2 µg/ ml and

incubated on ice for 15 minutes. Unbound streptavidin-PE was removed by washing twice with ice-cold media and samples were analyzed using flow cytometry. In parallel, cells not treated with anti-mouse/rat CD29 (Integrin β1)-biotin were incubated with streptavidin-PE as a control. Since our aim is to biotinylate the cell surface, this immunofluorescence assay serves to demonstrate adequate β1 expression, successful cell biotinylation, and availability of conjugated biotin for streptavidin binding.

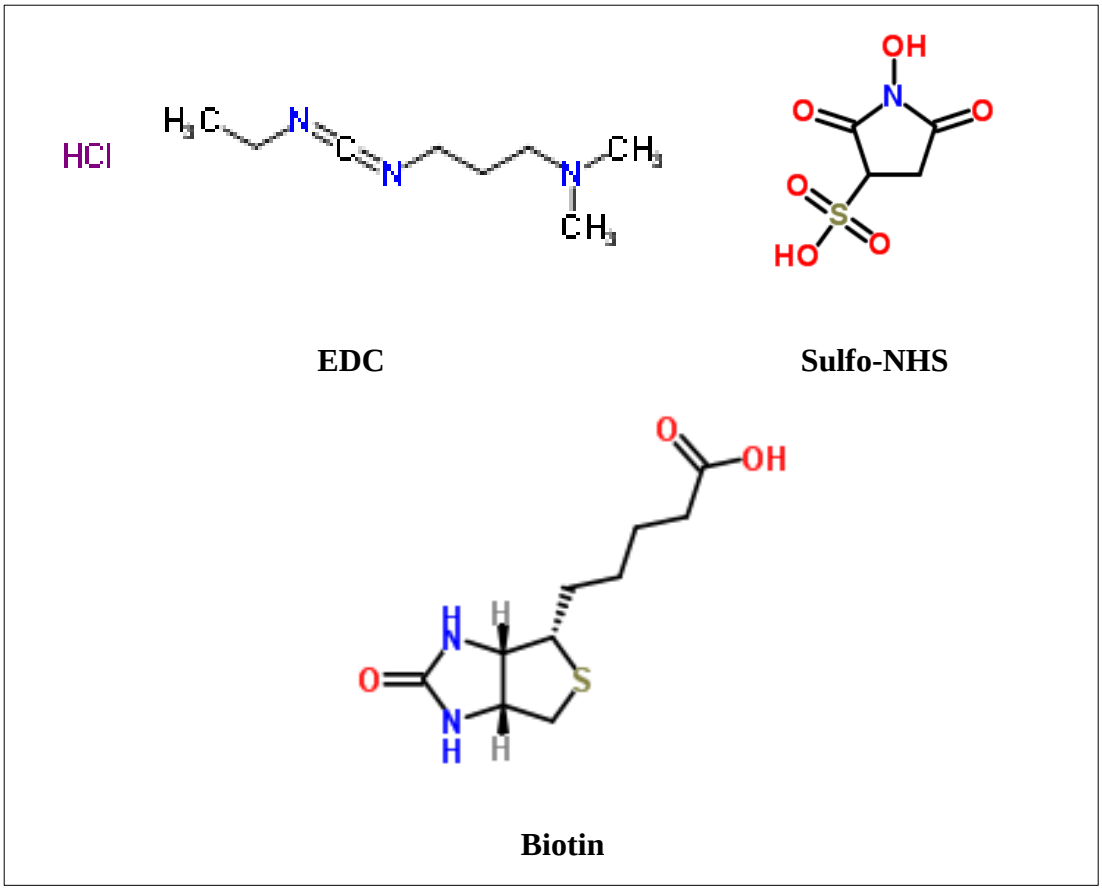

Figure II.2: Chemical structures of EDC, Sulfo-NHS, and Biotin.

Source: EDC: CSID:2006116, http://www.chemspider.com/Chemical-Structure.2006116.html (accessed Apr 21, 2013) [97], Sulfo-NHS: CSID:118082, http://www.chemspider.com/Chemical-Structure.118082.html (accessed Apr 21, 2013), Biotin: CSID:149962 [98], http://www.chemspider.com/Chemical-Structure.149962.html (accessed Apr 21, 2013) [99]

Cell-particle assembly

Basic cell-particle hybrid assembly

Rhodamine-labeled streptavidin-coated PLGA particles were incubated with biotinylated cells using different approaches at a starting particle:cell ratio of 1 mg particles: 5×10^5 cells/sample. Our first attempt involved a pilot study where streptavidin-coated PLGA particles were incubated with biotinylated cells for 15 minutes on ice followed by 5 or 15 minutes at 37°C after which samples were run on the flow cytometer and hybrids were detected by observing increased rhodamine fluorescence of cells as they bound to particles. This study involved two sets of samples: 1) adherent cells and 2) suspended cells. Two controls were set up; non streptavidin-coated PLGA particles incubated with biotinylated cells and streptavidin-coated particles incubated with non-biotinylated cells. Further successful assembly confirmation and investigation of incubation protocol was carried out next. To elaborate, we assembled cell-particle hybrids by incubating streptavidin-coated particles with biotinylated cells for A) 30 minutes on ice, B) 15 minutes on ice followed by 15 minutes at 37°C, or C) 15 minutes on ice followed by 30 minutes at 37°C. Based on results from previous experiments, we chose to use streptavidin-coated particles incubated with non-biotinylated cells as a control.

To eliminate the ambiguity of the flow cytometer results (flow cytometry cannot distinguish between particle/rhodamine uptake and particle binding), we also examined the assembled cell-particle hybrids microscopically using SEM and laser scanning confocal microscopy.

For confocal imaging, test and control samples were fixed in 4% paraformaldehyde and centrifuged onto slides using a cytospin (Cytospin®3, Shandon Scientific LTD, UK) at 700 rpm for 7 minutes. Cover slides were then mounted using Vectasheild mounting media with DAPI (Vector Laboratories, Inc. Burlingame CA).

Samples were imaged using Zeiss 710 confocal microscope (Carl Zeiss Microscopy, Thornwood, NY) using differential interference contrast (DIC)/fluorescence mode.

For SEM imaging, samples and controls were fixed in glutaraldehyde (EM grade, Electron Microscopy Science, Hatfield PA) and mounted on poly-L-lysine treated silica wafers. Samples were stained with osmium tetraoxide (Electron Microscopy Science, Hatfield PA) and gradually dehydrated with ethanol and HMDS (Hexamethyldisilazane, Polysciences Inc, Warrington PA). Samples were sputter coated with gold-palladium for 3 minutes prior to imaging on SEM at 2 kV accelerating voltage.

Effect of varying particle:cell ratio on the extent of particles binding to cell surface

Using the incubation protocol optimized earlier, we examined the possibility of conjugating more particles per cell. Rhodamine-loaded streptavidin-coated PLGA particles were incubated with biotinylated B16.F10 cells at a particle:cell ratio of 1 mg and 5 mg particles per 5×10^5 cells/sample for 15 minutes on ice followed by 15 minutes at 37°C. As a control rhodamine-loaded streptavidin-coated PLGA particles were incubated with non-biotinylated cells. Samples were run on the flow cytometer for analysis. Samples were also fixed for confocal imaging as described in the previous section.

Optimization of irradiation level and the effect of irradiation on the assembled hybrid

To better select the irradiation level to be used in the proposed hybrid vaccine system, we initially irradiated the cells with γ irradiation at 15, 30, and 45 Gy and then for a subsequent experiment at 35, 50, 75 Gy using a Cesium source (81-16A Cesium 137 irradiator. J.L. Shepherd & Associates, San Fernando, CA) at a rate of 26.2 Gy/min. B16.F10 cells at density of 5×10^5 cells/sample were irradiated as single cell suspensions

and then subsequently cultured to monitor cell growth and compared to non-irradiated cells as a control.

The ability of irradiated B16.F10 cells to form tumors in vivo was tested by challenging mice with cells irradiated at different levels and then mice were monitored for tumor growth over time. Specifically, four groups of mice (C57Bl/6 males more than 3 months old, 4 mice per treatment group, Jackson Laboratory, Bar Harbor, ME) were challenged with 10^5 cells/mouse. B16.F10 cells were irradiated with 35, 50, and 75 Gy. As a control mice were challenged with non-irradiated tumor cells. Tumor cells were injected subcutaneously in the shaved left dorsal flank. Animals were monitored over time for tumor growth. Animal handling and use was done according to University of Iowa Institutional Animal Care and Use Committee guidelines. When needed, animals were anesthetized using a ketamine/ xylazine mixture at 87.5mg/kg ketamine and 2.5mg/kg xylazine in 100 µl (intraperitonial injection). Animals were sacrificed (when tumor diameter reached 20 mm in diameter in any direction) using a CO_2 chamber followed by cervical dislocation.

To examine the stability of the assembled cell-particle hybrids to irradiation, we irradiated an assembled hybrid at the highest irradiation level tested (75 Gy). Rhodamine-labeled streptavidin-coated particles were incubated with biotinylated B16.F10 cells at a ratio of 1 mg particles:5×10^5 cells for 15 minutes on ice followed by 15 minutes at 37°C. As a control, rhodamine-labeled streptavidin-coated particles were incubated with non-biotinylated cells in parallel. Irradiated hybrids versus non-irradiated hybrids were examined using flow cytometry and confocal microscopy.

Applicability of the established cell-particle assembly method to other cell lines

We wanted to determine whether the established cell-particle hybrid manufacturing method described for B16.F10 cells could also be used successfully with a

different cell line. To demonstrate this, we chose to use RM11 cells, a prostate cancer cell line (a generous donation from Professor David Lubaroff, University of Iowa, Iowa city, IA). An immunoflourescence assay was performed similar to that of B16.F10 cells to examine expression of β1 integrin on the cell surface and successful cell biotinylation. In short, cells were trypsinized and washed twice with media and suspended in ice cold media at a concentration of 2×10^6 cells/ml, anti-mouse/rat CD29 (β1 integrin)-biotin was added at a final concentration of 5 µg/ml. Cells were incubated for 25 minutes on ice. Excess antibody was removed by washing twice using cold media. Streptavidin-PE was added at a final concentration of 2 µg/ml and incubated on ice for 15 minutes. Unbound streptavidin-PE was removed by washing twice with cold media and samples were run through a flow cytometer for analysis. In parallel cells not treated with anti-mouse/rat CD29 (β1 integrin)-biotin were incubated with streptavidin-PE as a control. Cell-particle hybrids were assembled by incubating rhodamine-labeled streptavidin-coated particles with biotinylated cells at particle to cell ratios of 1 and 5 mg particles:5×10^5 cells/sample for 15 minutes on ice followed 15 minutes at 37°C. As a control, rhodamine-labeled streptavidin-coated particles were incubated with non-biotinylated cells in parallel. Samples were run on the flow cytometer for analysis. Samples were also fixed for confocal imaging as described earlier (see page 27).

Statistical analysis

All experiments were performed at n = 3 unless otherwise stated. Results are presented as mean ± standard deviation. Student t-test or one way ANOVA analysis of variance followed by Tukey's post-testing were used to analyze differences between or among groups as data permits. Differences were considered significant at $p < 0.05$. Statistical analyses were performed using Prism software (GraphPad software Inc, San Diego, CA).

CHAPTER III: RESULTS

Particle preparation and processing

Particle characterization

PLGA particles were prepared by a double emulsion solvent evaporation method followed by a two-step differential centrifugation (see method page 20 for details). All particles used in this project were recovered from the pellet at the second centrifugation step of 10000 ×g for 10 minutes. Prepared particles were either: 1) CpG-loaded; 2) rhodamine-loaded; or 3) unloaded (blank) particles. Analysis of recovered particles of all three types by scanning electron microscopy (SEM: Figure III.1/ Table III.1) and Zetasizer measurements (Table III.1) revealed smooth surface and narrow size distribution respectively, with mean diameters of approximately 500 nm. We also imaged streptavidin-coated blank PLGA particles to examine surface morphology changes due to coating. No significant differences in size or charge were found between the three types of particles which justified the use of blank or rhodamine particles instead of expensive CpG-loaded particles, initially, for basic "proof of principle" experiments where the function of CpG was not needed. Recovered particles at the stated particle size (retrieved at the second centrifugation step) represented 33.42 ± 4.3 % of total weight of all particles recovered from both centrifugation steps (see equation II.1).

CpG loading and release kinetics

For the CpG-loaded particles prepared as described earlier, average CpG loading was found to be 1.63± 0.93 µg/mg particles which represents a loading efficiency of 10.87 % (n=3). These particles exhibited a large burst release with approximately 30% being released in the first 3 hours, and approximately 80% of the loaded CpG released by 12 hours. No further release of CpG was detected for the remaining course of the release study (Figure III.2).

Table III.1: Size and zeta potential of prepared particles

Particles	Diameter ± SD (nm)		PDI[c]	Zetapotential (mV)
	SEM[a]	Zetasizer[b]		
CpG loaded	504.81 ± 198.36	536.72 ± 64.39	0.12 ± 0.05	- 28.40 ± 0.29
Blank	486.38 ± 136.86	527.4 ± 33.68	0.20 ± 0.09	- 26.50 ± 5.26
Rhodamine loaded	452.75± 131.61	NA	NA	- 26.23 ± 2.03

a: Particle size measured from SEM images using ImageJ software, n = 100

b: Particle size measured using zetasizer, n = 3.

c: Polydispersity index

NA: not applicable

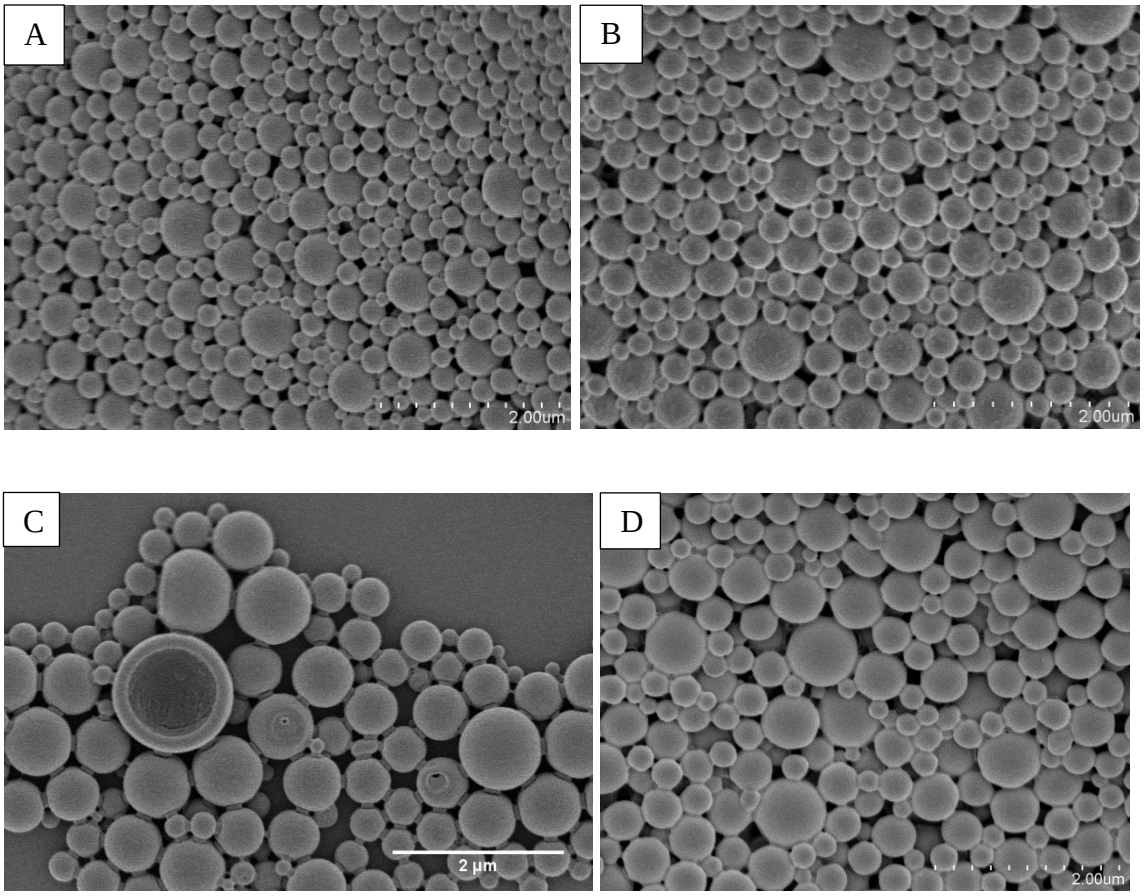

Figure III.1: SEM images of A: blank particle, B: rhodamine-loaded particle, C: CpG-loaded particle, D: streptavidin surface-modified particles. All particles were imaged after lyophilization. Particles were coated with gold-palladium prior to imaging at 2 kV acceleration voltage. Scale bar = 2 µm.

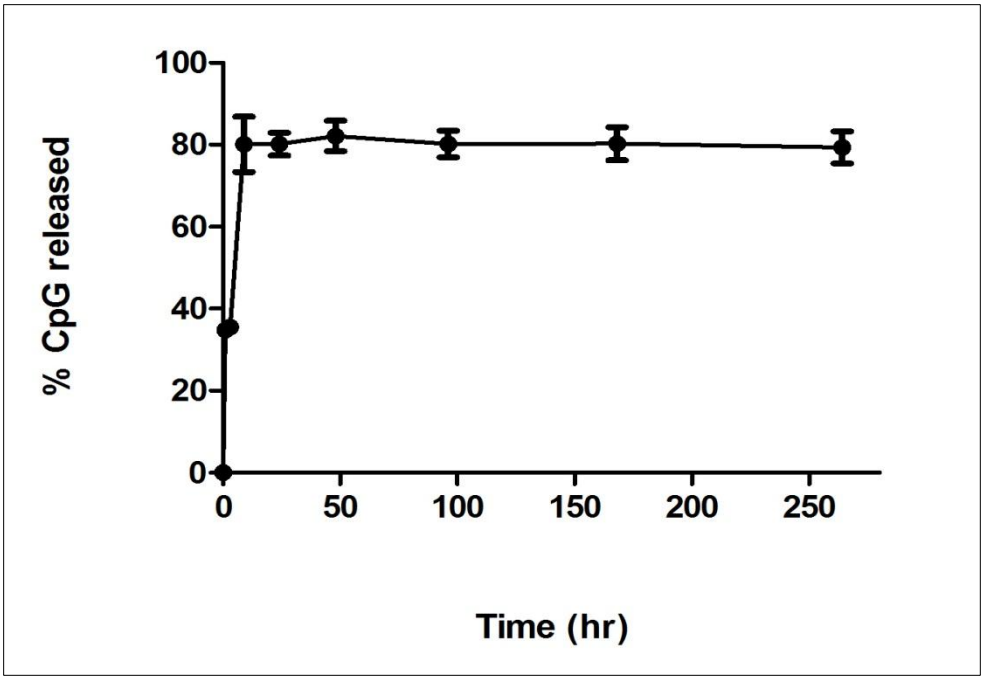

Figure III.2: In vitro release profile of CpG-loaded particles. Each sample was 25 mg of CpG-loaded particles that was suspended in PBS, pH 7.4 and incubated on a rotary shaker at 37°C. Measurements were taken at several time points and samples were analyzed using OliGreen® fluorescence kit, n = 3.

Surface conjugation of streptavidin to PLGA particles

Blank PLGA particles, prepared as described earlier, were treated with EDC/NHS to activate surface carboxylic acid groups (see method page 23). Then the ability of surface-activated PLGA particles to form amide linkages with streptavidin-PE was assessed using fluorescently labeled streptavidin (streptavidin-PE). To confirm that binding was mediated by amide linkages we set up the two following controls: 1) we incubated streptavidin-PE with blank PLGA particles that were not surface activated with EDC/NHS and; 2) we incubated surface-activated blank PLGA particles with BSA (as blocking agent) followed by streptavidin-PE. The results demonstrated specific streptavidin-PE binding as indicated by higher levels of PE fluorescence by EDC/NHS treated particles versus controls (Figure III.3).

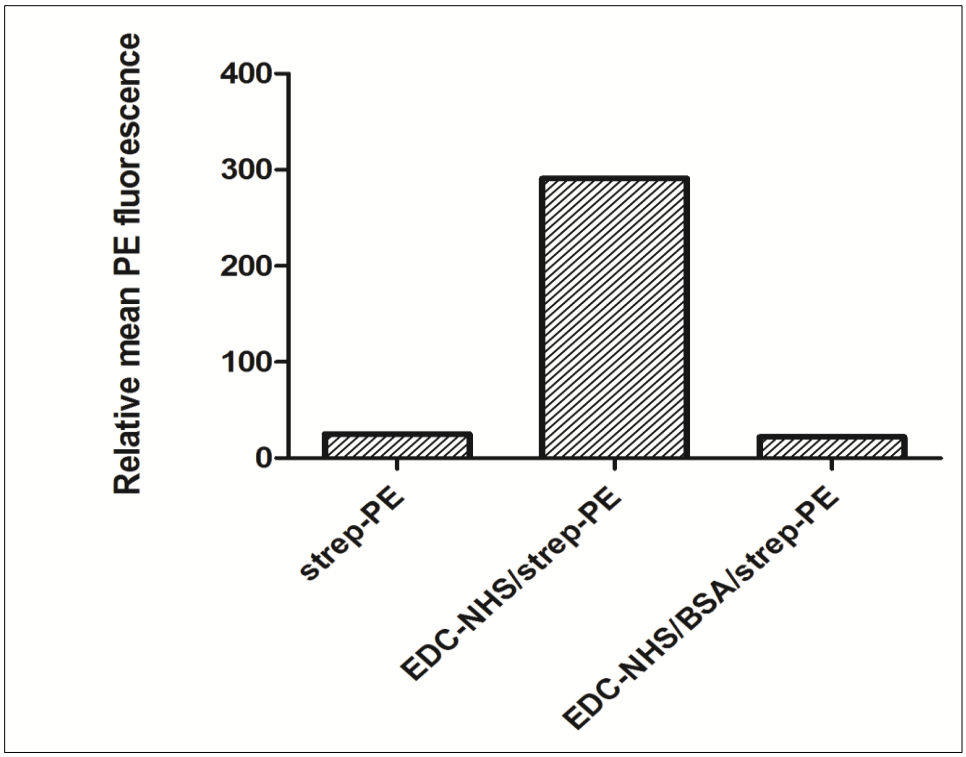

Figure III.3: Surface conjugation of streptavidin-PE on PLGA particle surface via amide linkages. Blank PLGA particles were treated with EDC/NHS and then incubated with streptavidin-PE (EDC-NHS/strep-PE). As a control, EDC/NHS treated particles were blocked with BSA prior to adding streptavidin-PE (EDC-NHS/BSA/strep-PE); or non-EDC/NHS treated particles were incubated with streptavidin-PE (strep-PE). All samples were run on a flow cytometer for analysis (n = 1/treatment group).

Thus far, results revealed our ability to surface conjugate streptavidin to PLGA particles using amide linkages, however, the amount of streptavidin-PE added was based on product instructions for detection of biotinylated substrates. Therefore we wanted to determine if we needed to increase the amount streptavidin in order to saturate the particle surface. The range examined was 0.06 - 0.3 μg/mg particles and 0.3 - 8 μg/mg particles in two separate experiments. As can be seen from Figures III.4 and III.5, PE fluorescence increases with increasing amounts of streptavidin-PE added. Since 4 μg of streptavidin/mg particles demonstrated good increment in streptavidin binding as

detected by PE fluorescence and we wished to save on this reagent we chose this quantity for future experiments involving cell-particle hybrid assembly.

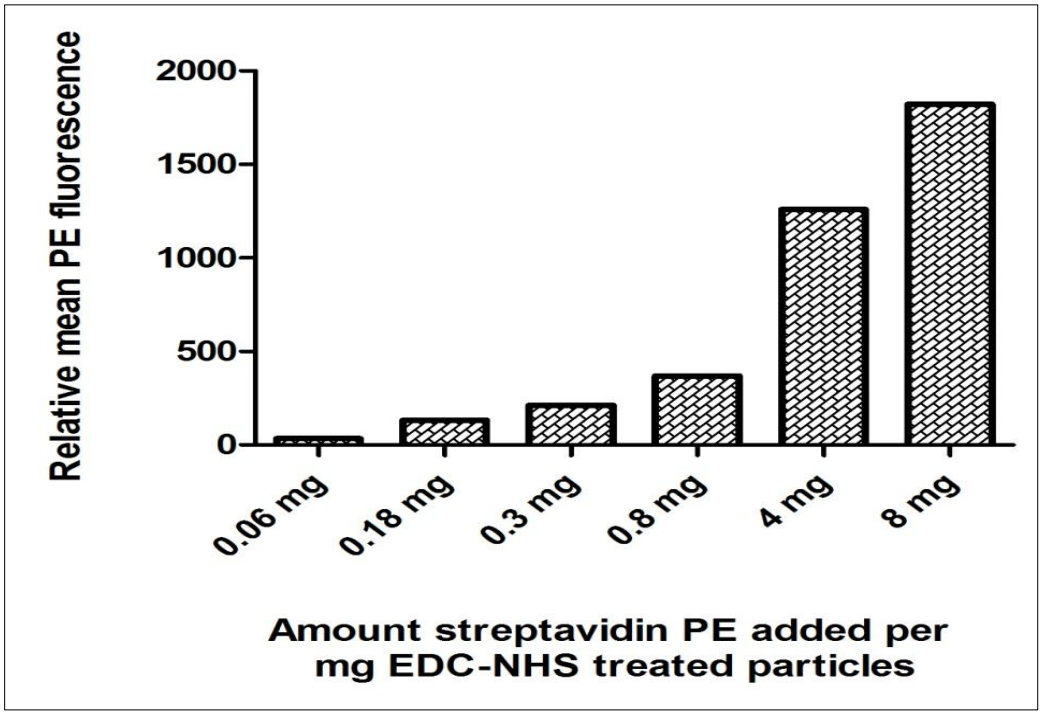

Figure III.4: Relative mean PE-fluorescence of streptavidin-PE coated PLGA particles for a range of added streptavidin-PE. Blank PLGA particles were treated with EDC/NHS prior to incubation with increasing amounts of streptavidin-PE in the range of 0.06 - 8 μg/mg particles. Samples were run on a flow cytometer for analysis. Data represents pooled results of two experiments (n = 1/treatment group).

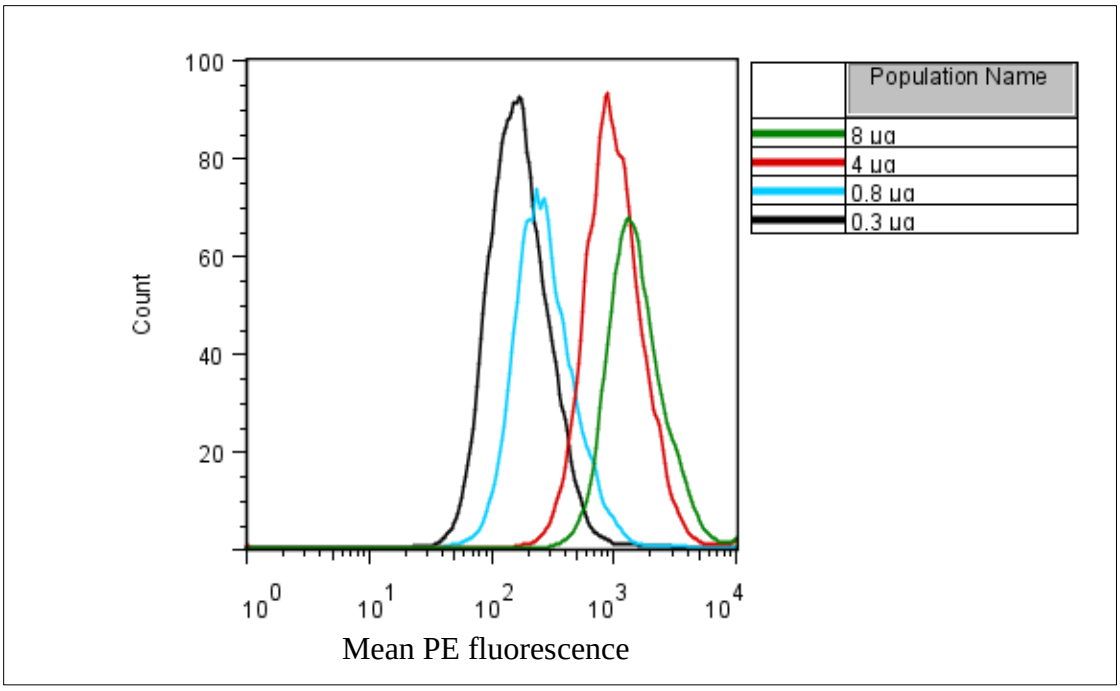

Figure III.5: Flow cytometer histograms of particles surface-conjugated with increasing amounts of streptavidin-PE in the range of 0.3 - 8 µg/mg particles. Blank PLGA particles were treated with EDC/NHS and then incubated with increasing amounts of streptavidin PE. Samples were run on a flow cytometer for analysis (n = 1/treatment).

Prior to assembling cell-particle hybrids using avidin-biotin linkages, we wished to assess the ability of conjugated streptavidin to bind biotin. Thus we coated unloaded (blank) EDC/NHS treated PLGA particles with unlabeled streptavidin and then incubated these streptavidin-coated particles with fluorescein-linked biotin. We then measured the fluorescein fluorescence signal of the tested particles, using flow cytometry, as an indication of successful avidin-biotin binding. To eliminate the possibility that the measured signal was due to non-specific binding of fluorescein-biotin to free reactive carboxylic groups on the particles that might not be linked to streptavidin, we incubated EDC/NHS treated blank particles directly with fluorescein-biotin. Results showed that streptavidin was available for biotin binding and that biotin binds to streptavidin-coated particles to a significantly higher level than to EDC/NHS-treated particles (Figure III.6).

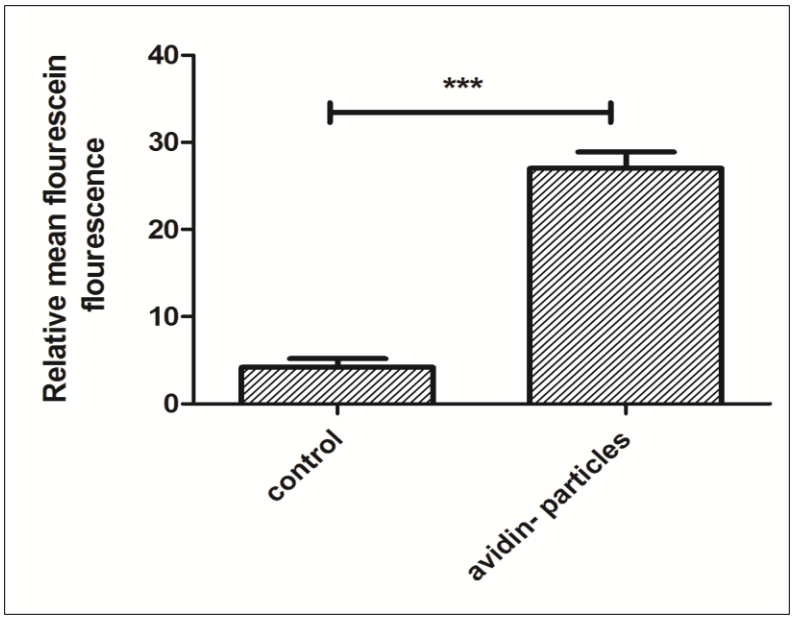

Figure III.6: Binding of streptavidin surface-modified particles to biotin fluorescein. Fluorescence intensities were measured using flow cytometry. Legend: Control = EDC/NHS treated particles incubated with biotin fluorescein directly; avidin-particles = streptavidin coated particles incubated with biotin fluorescein. *** $p < 0.001$, n = 3.

These results revealed the ability of the surface modified PLGA particles to bind biotin making those particles potential candidates for surface engineering of biotinylated tumor cells, one of the primary goals of this project.

Effect of surface modifying PLGA particles on the loaded CpG levels

As stated earlier, the initial CpG loading of the fabricated PLGA particles was 1.63 ± 0.93 µg/mg particles, which was very low. Subsequent surface modification of these particles involves aqueous incubations and washes that could further reduce the final amount of CpG remaining entrapped. To estimate CpG loss during the surface modification process, we treated CpG-loaded particles with EDC/NHS and then coated these particles with streptavidin. These streptavidin-coated CpG-loaded particles were

degraded to measure the amount left relative to the original loading (see method equation II.4). As expected, the process of surface modifying particles with streptavidin resulted in a significant loss of loaded CpG which was estimated to be 80% of the total encapsulated amount. However, we also looked at whether the remaining CpG is still available for release. We carried out an in vitro release study using streptavidin surface-coated CpG-loaded particles under the same conditions as performed earlier with the unmodified CpG particles. The release study showed that streptavidin surface modified particles were still capable of releasing detectable amounts of CpG (Figure III.7).

Antibody-mediated cell surface biotinylation

Having succeeded in coating PLGA particles with functionally active streptavidin, we then attempted to modify the other component of the cell-particle hybrid system (the cells) to be capable of efficiently binding the particles. We chose to coat the cells with biotin indirectly as our other attempts using the method reported in the literature using biotin hydrazide [94] failed to achieve cell-particle hybrids. Rather than investigating more into this method, we chose to biotinylate the cells using a commercially available biotin-linked antibody specific for the ubiquitously expressed cell surface protein β1 integrin (CD29) [100]. Using the murine melanoma cell line B16.F10, we confirmed that β1 integrin surface expression by these cells could be detected using a direct immunofluorescent technique involving the biotin-labeled anti-β1 integrin antibody. Binding of this antibody was determined using streptavidin-PE and running the samples through a flow cytometer. The same experiment was repeated with a murine prostate cancer cell line, RM11, to demonstrate the general applicability of the cell-particle binding method described here. Results showed readily detectable levels of cell surface expression of β1 integrin for both cell lines tested (Figure III.8). As our goal is to biotinylate the cell surface, this immunofluorescent assay also serves to confirm successful cell surface biotinylation and the availability of the conjugated biotin for

streptavidin binding. Results showed that cells were efficiently biotinylated and the conjugated biotin was available for streptavidin binding.

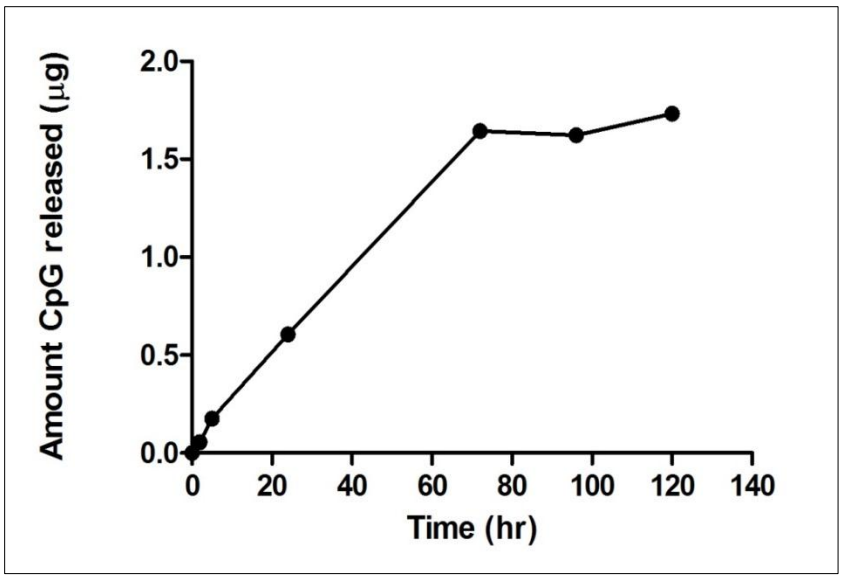

Figure III.7: Release profile of CpG from streptavidin surface modified CpG-loaded particles. Streptavidin-coated CpG-loaded particles (10 mg) were suspended in PBS, pH 7.4 and incubated on a rotary shaker at 37°C. Measurements were taken at several time points and samples were analyzed using OliGreen® fluorescence kit, n = 1.

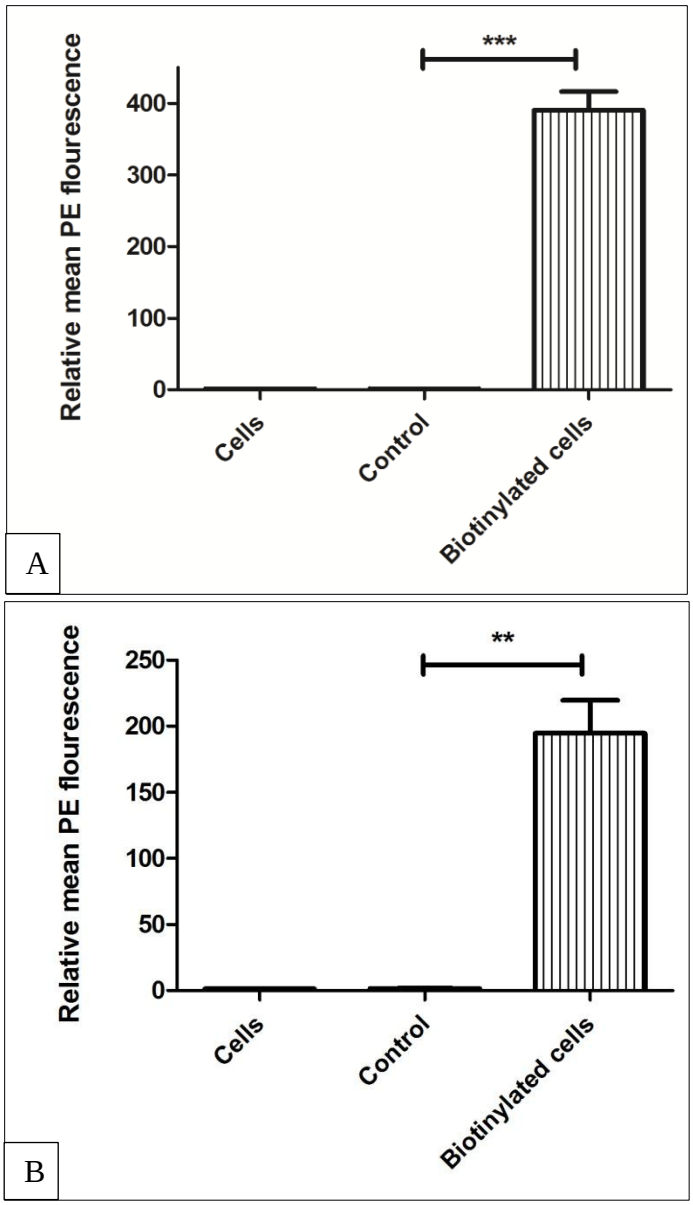

Figure III.8: Detection of β1 integrin expression on B16.F10 cells (A) and RM11 cells (B) using biotinylated anti-β1 antibodies. Measurements of fluorescence intensity were made using flow cytometry. Legend: cells = non-biotinylated cells with no streptavidin-PE incubation; control = non-biotinylated cells incubated with streptavidin-PE; biotinylated cells = cells treated with biotinylated anti-β1 antibody and incubated with streptavidin-PE. n = 3, ** $p < 0.01$, *** $p < 0.001$.

Cell-particle hybrid assembly

Cell-particle hybrids were assembled by binding PLGA particles to cells using avidin-biotin linkages. Rhodamine-labeled PLGA particles (prepared as described in methods page 20) were surface-coated with streptavidin after being treated with EDC/NHS (see method page 23). B16.F10 cells were surface biotinylated indirectly using biotin-tagged anti-β1 antibody. In a pilot study PLGA particles and cells were mixed at a particle:cell ratio of 1 mg particles:5×10^5 cells and incubated under varying conditions as explained below. Initially, we set up two controls; non-biotinylated cells incubated with streptavidin-coated particles and biotinylated cells incubated with non-coated particles. After the incubation, samples were run through the flow cytometer to determine the degree of cell:particle assembly. Data were analyzed (using FlowJo® software) by gating on the cells (or cell-particle hybrids) in a dot-plot (forward scatter (FSC) versus side scatter (SSC)) and generating a histogram denoting the relative fluorescence (rhodamine) of each treatment group from which mean values were obtained (Figure III.9).

Since B16.F10 cells are adherent cells, it was necessary to look at the best approach to process the cells; either as adherent cells or as single cell suspensions. Thus, in an initial pilot experiment, cells were biotinylated while adherent and compared to biotinylated single cell suspensions. Cells treated in suspension showed more efficient particle binding compared to adherent cells. Thus we decided to treat cells while in suspension in future experiments (Figure III.10). At our first attempt to assemble cell-particle hybrids, we found that incubating cells and particles for 20 minutes on ice does not result in binding at an acceptable level (data not shown). We therefore included a 37°C incubation time for 5 or 15 minutes immediately subsequent to 15 minutes incubation on ice. The ice-incubation time was kept in use as the starting treatment to prevent possible endocytosis of the biotinylated integrin-antibody complex that might result in losing cell-surface biotinylation. With this modification to the incubation

temperature, cell-particle hybrids were successfully assembled as demonstrated by higher relative mean rhodamine fluorescence intensity expressed by the biotinylated cell-streptavidin particle conjugates compared to negative controls (Figure III.10).

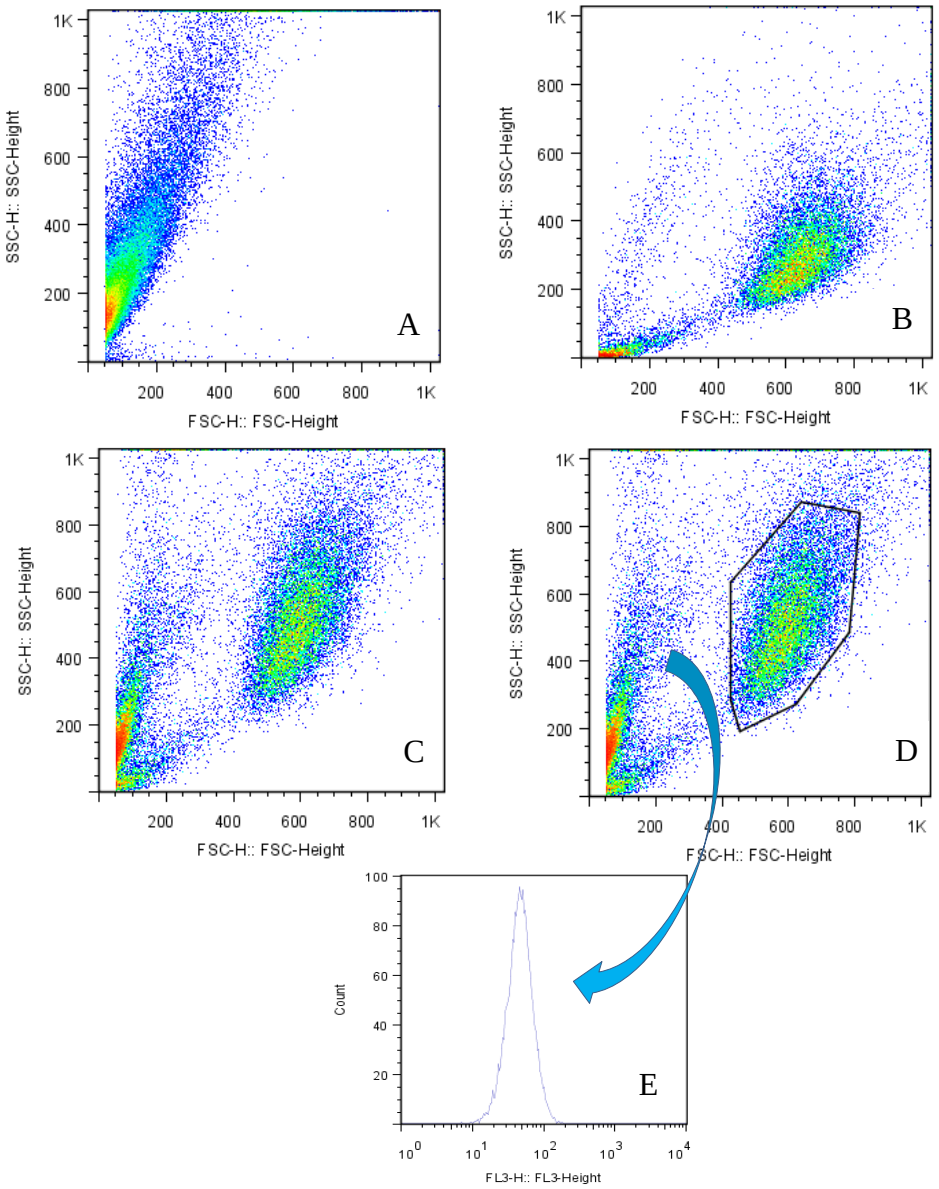

Figure III.9: Example of a flow cytometer dot-plot that shows the strategy for data analysis adopted in this project. (A): particles alone (suspended in cell culture media), (B): cells alone, (C): cell-particle mix, (D): gating on cells (or cell-particle hybrids) in (C) for analysis, (E): fluorescence (rhodamine) histogram generated for the gated population in (D).

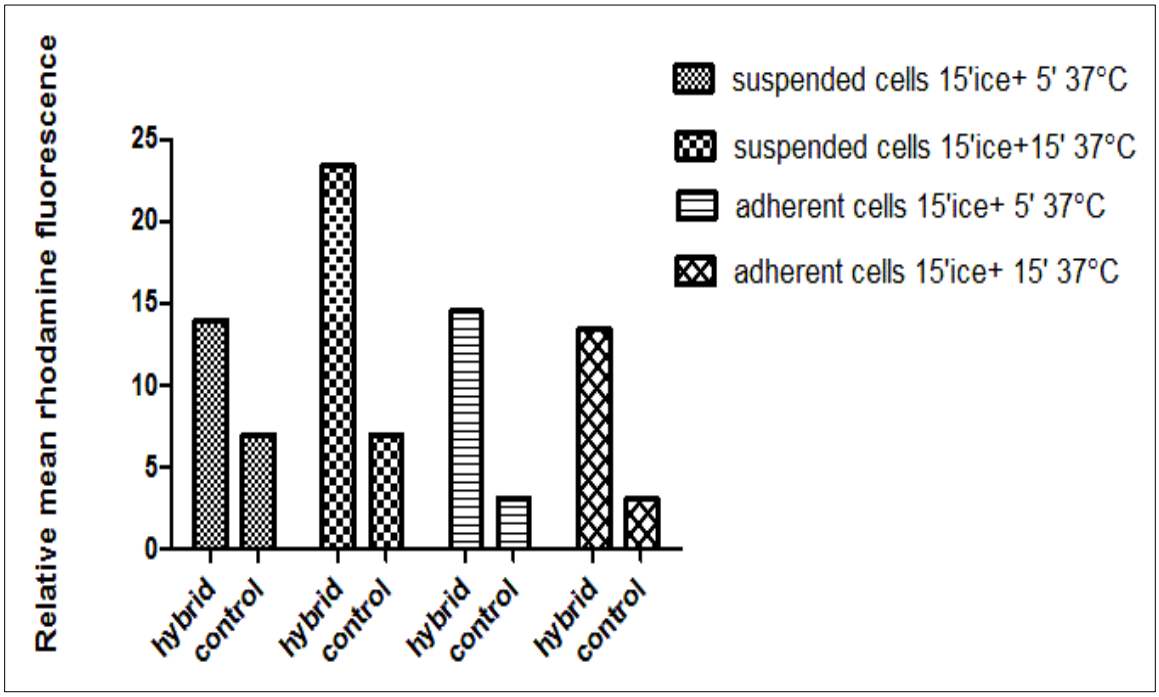

Figure III.10: Efficiency of assembling cell-particle hybrids using suspended cells compared to adherent cells. Fluorescence levels were measured using flow cytometry. Legend: Hybrid = biotinylated cells incubated with streptavidin coated particles; control = non-biotinylated cells incubated with streptavidin coated particles. Amount of particles in all samples was 1 mg. Suspended cells are 5 x 10^5 cells/sample. Adherent cells were 60% confluent cells in a 6 well plate, n = 1.

We also found that both controls showed similar results, thus we decided on only using non-biotinylated cells incubated with streptavidin coated particles as our control in future experiments (Figure III.11).

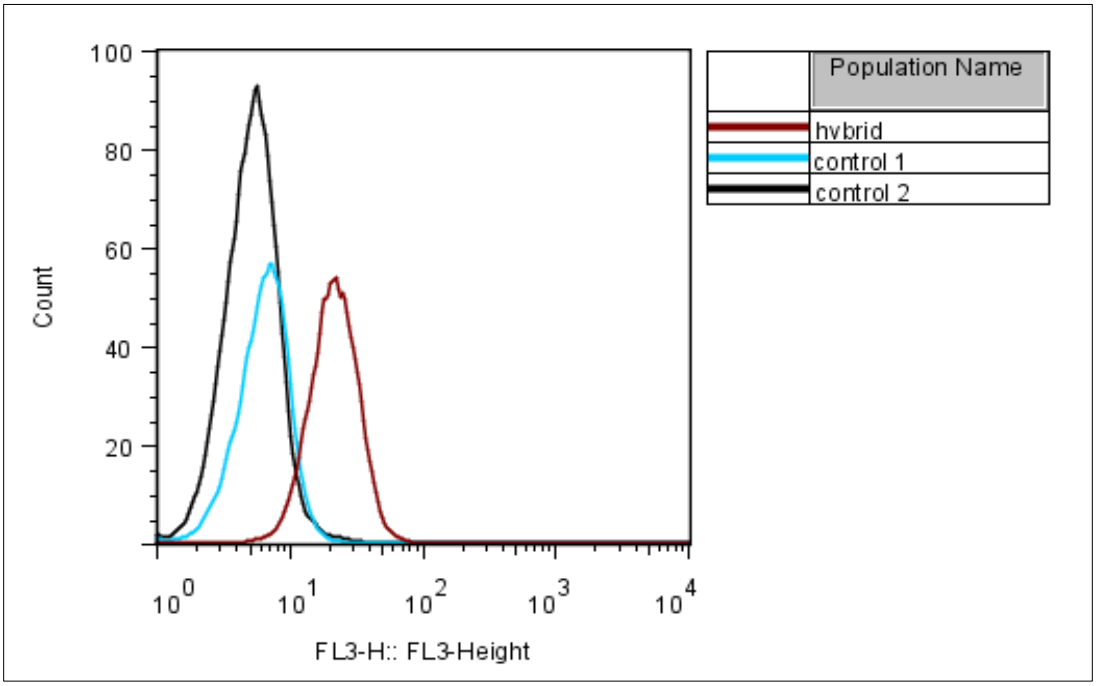

Figure III.11: Rhodamine fluorescence histograms (using flow cytometry) showing complete shift of the cell-particle hybrid population from the control. Legend: hybrid = biotinylated cells incubated with streptavidin coated particles, control 1 = non-biotinylated cells incubated with streptavidin coated particles, control 2 = biotinylated cells incubated with non-coated particles. All samples were incubated at a ratio of 1 mg particles:5 x 10^5 suspended cells/sample for 15 minutes on ice followed by 15 minutes at 37°C.

As we saw an increase in particle binding to cells with longer 37°C incubation we wanted to determine whether it was the longer time or the higher incubation temperature that was responsible. We increased incubation time on ice in one sample and included samples where we increased the time for incubation at 37°C to look at how that might alter the results. The control (non-biotinylated cells incubated with streptavidin-coated particles) for this experiment was incubated for 15 minutes on ice followed by 15 minutes at 37°C.

All incubation protocols showed significant increases relative to the control which means cell-particle hybrids were successfully assembled in all three protocols assayed. However, when we looked at differences in relative mean rhodamine fluorescence, a significant difference was evident only between hybrids assembled for 15 minutes on ice followed by 30 minutes at 37°C compared to hybrids assembled for 30 minutes on ice (Figure III.12). For future experiments we chose to work with 15 minute ice incubation followed by 15 minutes at 37°C as our incubation protocol as we considered the level of binding sufficient and wished to avoid possible particle uptake that might start taking place with longer incubations at 37°C.

In order to confirm that the results described above, obtained using flow cytometry, were likely due to the formation of cell-particle hybrids, we examined these mixtures using scanning electron microscopy (SEM) and laser scanning confocal microscopy (Figures III.13-III.14). Biotinylated cells (prepared as described above) were incubated with rhodamine-labeled streptavidin-coated PLGA particles for 15 minutes on ice followed by 15 minutes at 37°C at a particle:cell ratio of 1 mg particles:5×10^5 cells. The control used involved non-biotinylated cells incubated with rhodamine-labeled streptavidin-coated PLGA particles under the same conditions as used for test samples. Subsequently, samples were fixed with the appropriate fixative (see method pages 27-28) for the intended imaging (SEM or confocal microscopy).

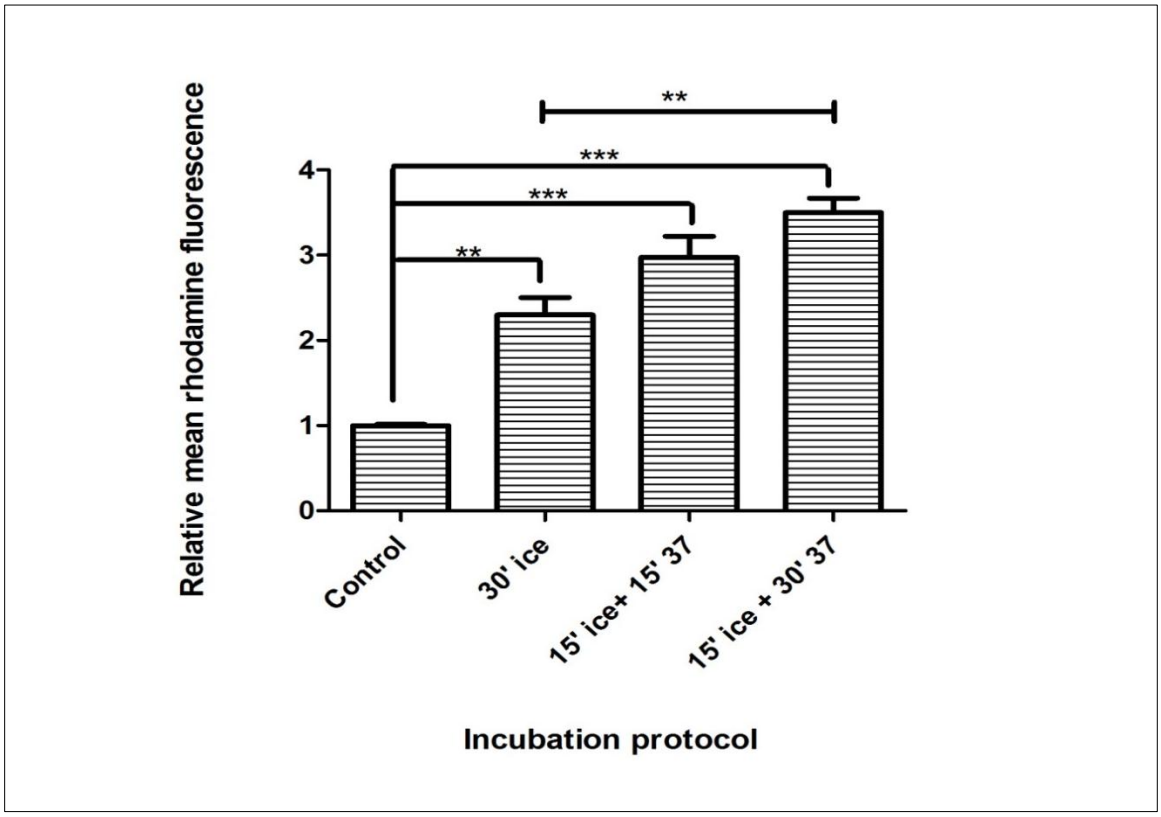

Figure III.12: Effect of incubation protocols on the efficiency of cell-particle hybrid assembly. Samples were biotinylated cells incubated with streptavidin coated particles loaded with rhodamine. Samples were assayed using flow cytometry. Control = non-biotinylated cells incubated with streptavidin coated particles for 15 minutes on ice followed by 15 minutes at 37°C. ** $p < 0.01$, *** $p < 0.001$. n = 3.

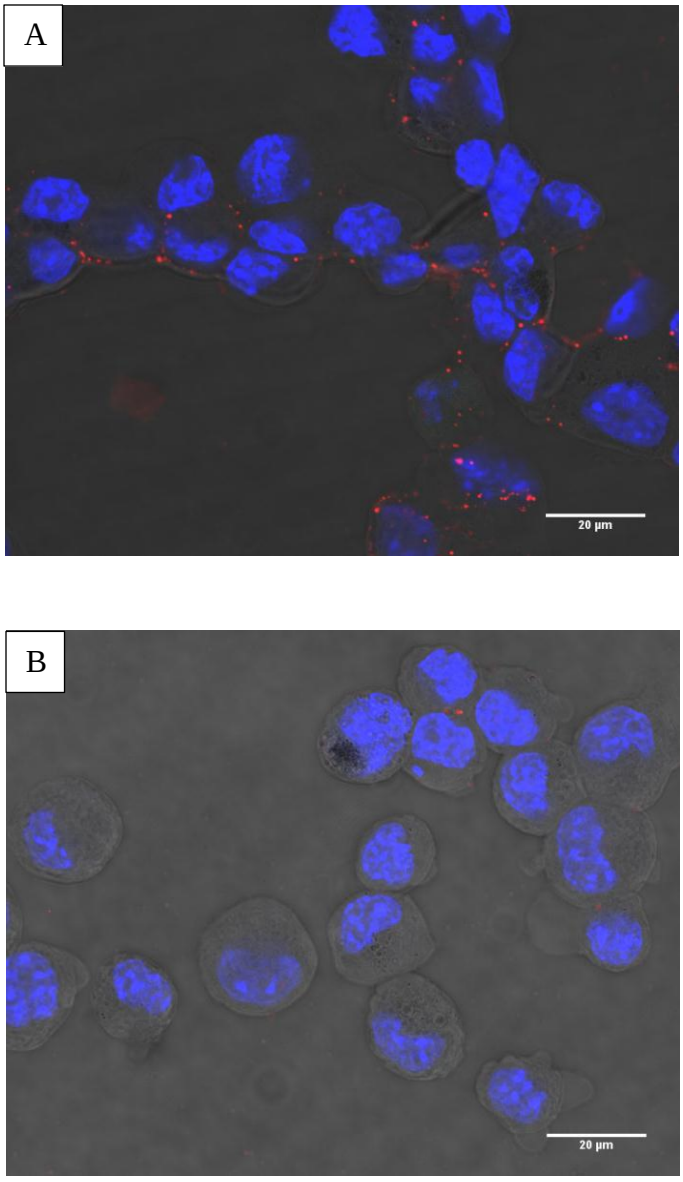

Figure III.13: Laser scanning confocal microscopy images of (A) cell-particle hybrids assembled when 1 mg rhodamine-labeled streptavidin-coated PLGA particles were incubated with 5×10^5 biotinylated cells for 15 minutes on ice followed by a 15 minute incubation at 37°C and (B) negative control involved incubating rhodamine-labeled streptavidin-coated PLGA particles with non-biotinylated cells at same conditions as in (A). Samples were fixed in 4% paraformaldehyde and imaged using DIC/ fluorescence mode at 63 X magnification. Blue: DAPI stained cell nuclei, Red: rhodamine-labeled PLGA particles. Scale bar = 20 µm.

Figure III.14: SEM imaging of: cell-particle hybrid (A), (B): negative control (C), (D) and non-biotinylated B16.F10 cells that were not incubated with particles (E). Test samples were rhodamine labeled streptavidin-coated particles incubated with biotinylated cells at a ratio of 1 mg particles:5×10^5 cell for 15 minutes on ice followed by 15 minutes incubation at 37°C. Controls were non-biotinylated cells incubated with rhodamine-labeled streptavidin-coated particles at same conditions as test samples. Samples were fixed with glutaraldehyde and gradually dehydrated with ethanol and HMDS and coated with gold-palladium prior to imaging at 2 kV accelerating voltage. Scale bar: A, C and E = 10 micron, B and D = 5 micron.

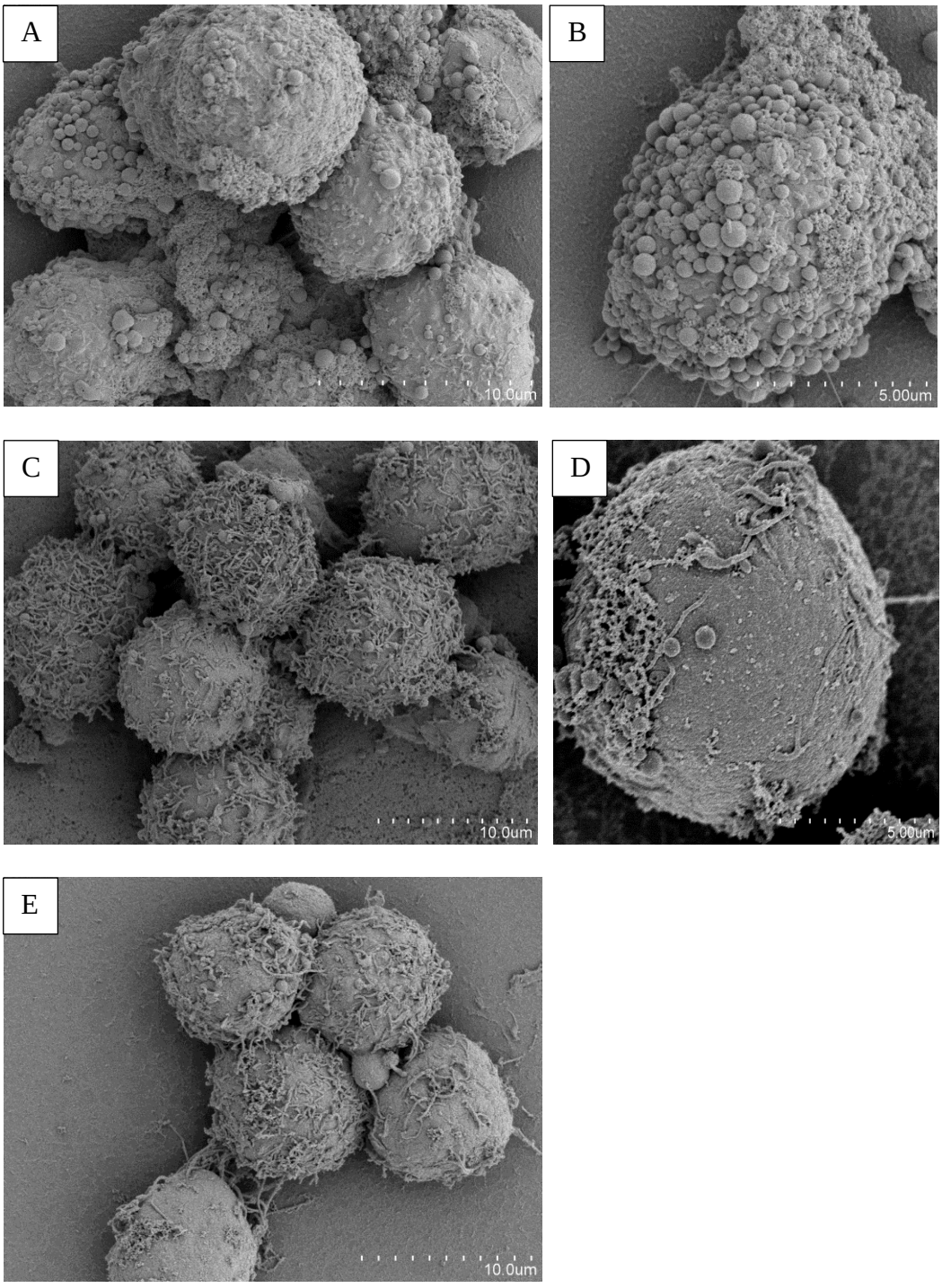

Effect of varying particle:cell ratio on the extent of particles binding to cell surface

After confirming successful particle binding to the cell surface of the melanoma cell line, and having selected the incubation time and temperature to use in upcoming experiments, we then optimized the ratio of particles:cells to use. We increased the particle:cell ratio in five-fold amounts and looked at the extent of cell-particle hybrid assembly as determined by flow cytometry and confocal microscopy. Rhodamine-labeled streptavidin-coated particles were incubated with biotinylated cells at a particle:cell ratio of 1 and 5 mg particles per 5×10^5 cells. As a negative control, non-biotinylated cells were incubated with rhodamine-labeled streptavidin-coated particles at the same particle:cell ratios stated above. Test samples and controls were incubated on ice for 15 minutes followed by 15 minutes at 37°C after which they were run through a flow cytometer where the level of rhodamine fluorescence associated with cells was measured to indicate the degree of cell-particle binding. To corroborate the findings from flow cytometry, test samples and controls were fixed and imaged using laser scanning confocal microscopy.

The results showed that more particles were binding per cell when the particle dose was increased. This was evident by the high rhodamine fluorescence signal associated with cells incubated with 5 mg particles which was significantly higher than cells incubated with 1 mg particles. This finding was further confirmed by the significantly increased side scatter of the test samples treated with 5 mg particles versus 1 mg particles (Figure III. 15). Side scatter is a measure of cell granularity that is normally measured in particle uptake studies [101] and for our purposes, we looked at side scatter as an indication of increased cell granularity caused by the conjugated particles. The microscopic imaging of the samples and controls further supports the conclusion that more particles are binding per cell as the particle:cell ratio was increased (Figures III.16-III.17).

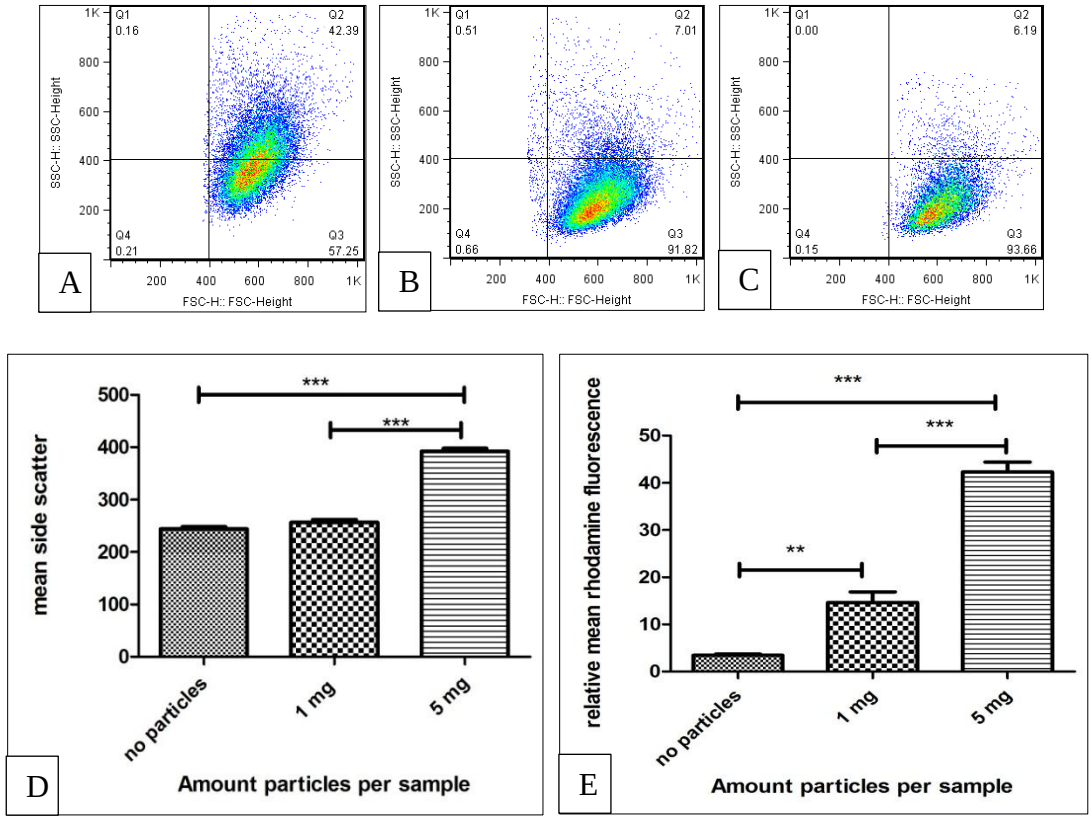

Figure III.15: Effect of particle:cell ratio on the extent of particles binding to B16.F10 cells. (A-C): Side scatter versus forward scatter dot plot of cell-particle hybrids assembled using varying particle:cell ratios. 5×10^5 biotinylated cell were incubated with (A): 5.0 mg, (B): 1.0 mg, (C): 0.0 mg rhodamine-labeled streptavidin-coated PLGA particle for 15 minutes on ice followed by 15 minutes incubation at 37°C prior to running through the flow cytometer. (D): Side scatter bar chart for the three treatments in (A-C), (E): relative mean rhodamine fluorescence of the three treatment groups in (A-C), for (E) data are presented as relative mean rhodamine fluorescence of test sample minus fluorescence level of control. ** $p < 0.01$, *** $p < 0.001$, n = 3.

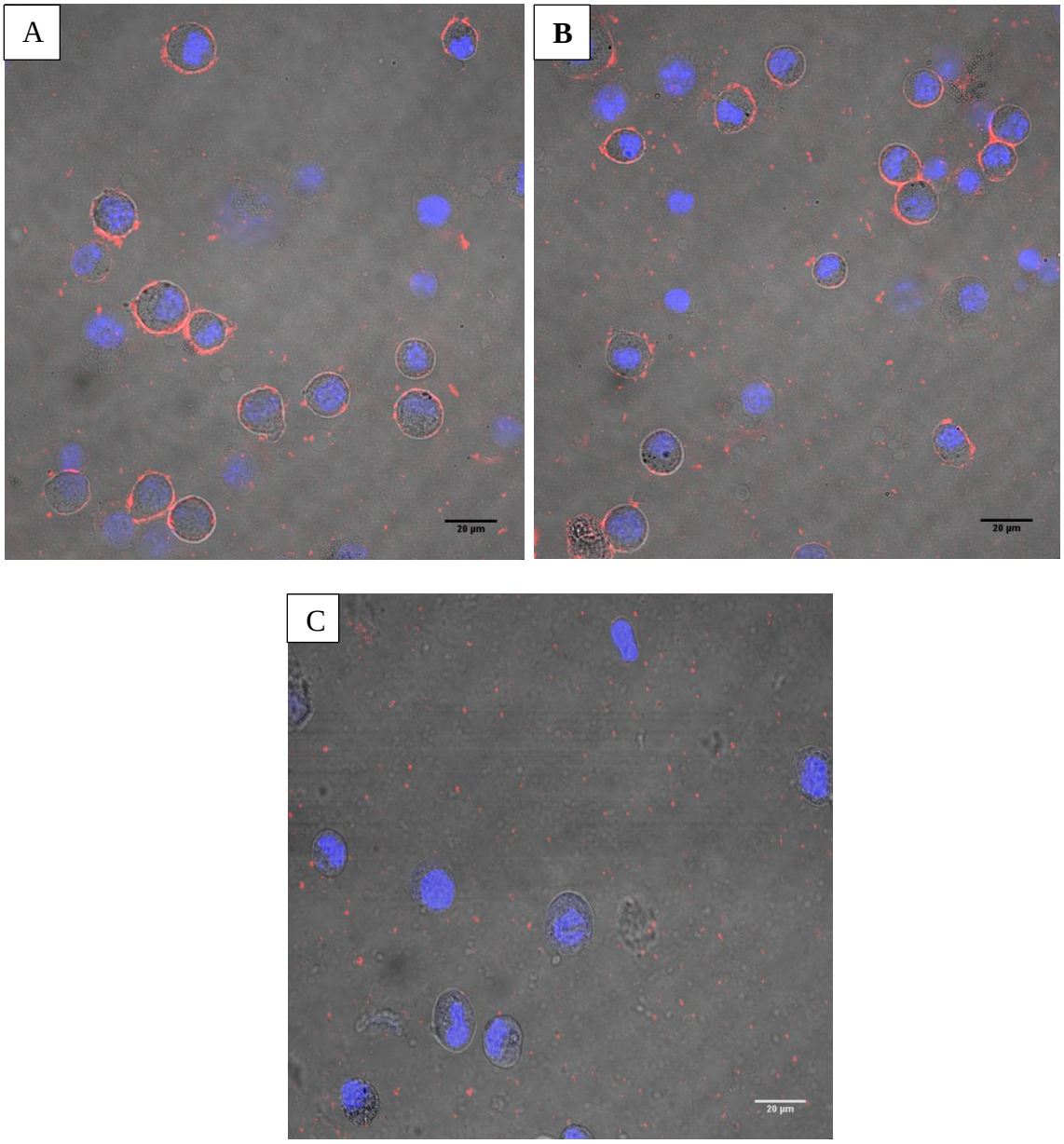

Figure III.16: Laser scanning confocal microscopy images of B16.F10 cell-particle hybrids assembled at a ratio of 1 mg particles per 5×10^5 cells. Test samples: rhodamine-labeled streptavidin-coated particles were incubated with biotinylated cells for 15 minutes on ice followed by 15 minutes incubation at 37°C then samples were fixed in 4% paraformaldehyde and imaged using DIC/fluorescence mode at 63X (A,B). Control samples: non-biotinylated cells that were incubated with rhodamine-labeled streptavidin-coated particles at same conditions as test samples (C). Blue = DAPI-stained cell nuclei, Red= rhodamine-labeled PLGA particles. Scale bar = 20 µm.

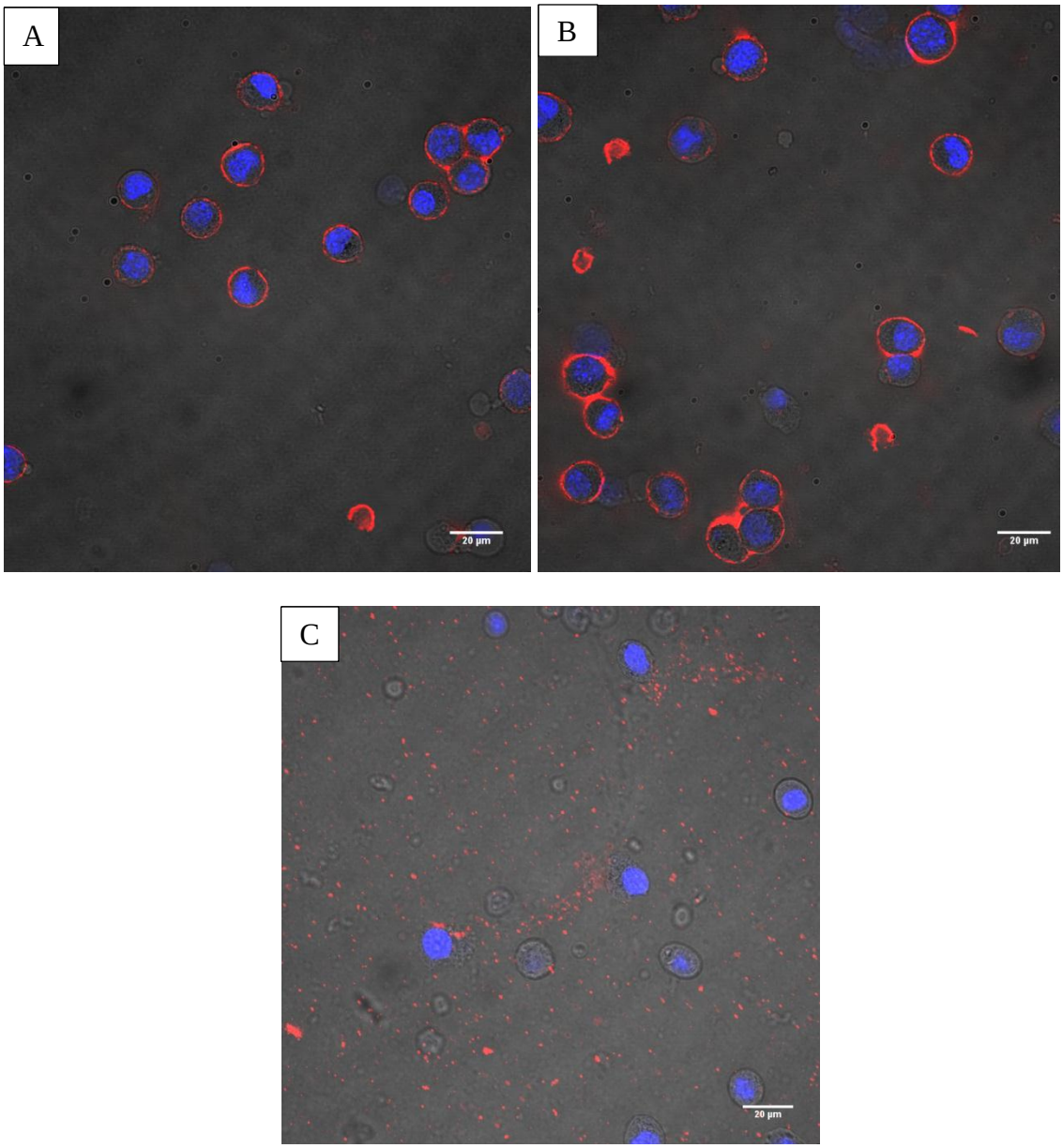

Figure III.17: Laser scanning confocal microscopy images of B16.F10 cell-particle hybrids assembled at a ratio of 5 mg particles per 5×10^5 cells. Test samples: rhodamine-labeled streptavidin-coated particle were incubated with biotinylated cells at the above ratio for 15 minutes on ice followed by 15 minutes incubation at 37°C then samples were fixed in 4% paraformaldehyde and imaged using DIC/fluorescence mode at 63X (A,B). Control samples: non-biotinylated cells that were incubated with rhodamine-labeled streptavidin-coated particles under the same conditions as test samples (C). Blue= DAPI-stained cell nuclei, Red= rhodamine-labeled PLGA particles. Scale bar = 20 µm.

Optimization of irradiation level and effect of irradiation on the hybrid assembly

We attempted to observe the optimum irradiation level to use that will abolish cell proliferation, yet does not cause cell death too rapidly. We monitored cell viability over time in vitro and tested the ability of the irradiated cells to cause tumors in vivo. For the in vitro experiments, we initially used 15, 30 and 45 Gy. This range was based on levels used by others for systems involving B16.F10 cells [58]. Cells irradiated at 15 Gy showed no big differences from control non-irradiated cells in terms of reaching confluence, in vitro, and they showed signs of continued in vitro growth 10 days after irradiation. Cells that received an irradiation dose of 30 Gy or greater were inhibited from proliferation but remained viable for up to 5 weeks. However, these assessments were based on simple microscopic monitoring of cell growth relative to non-irradiated control and did not involve any proliferation assays.

As the in vitro observations of irradiated cells' capacities to proliferate did not conclusively prove that all cells had been growth-inhibited, we also performed in vivo studies to test the ability of the irradiated cells to form tumors. Mice were challenged with 10^5 B16.F10 cells that had been irradiated with 0, 35, 50, and 75 Gy (4 mice per group). Five weeks subsequent to tumor challenge 3 out of 4 mice challenged with non-irradiated cells developed tumors that reached 20 mm in diameter and had to be sacrificed, while none of the mice challenged with irradiated tumor cells developed tumors. These results indicate that irradiation at all doses had possibly rendered cells non-carcinogenic and therefore we can use the lowest tested radiation dose for preparing irradiated cell-particle hybrid for future in vivo testing of our hypothesized cancer vaccine system.

Since there are no reports in the literature on cell-particle assemblies involving irradiated cells, we had no indication as to whether to irradiate cells before or after hybrid assembly. We chose to irradiate cells subsequent to assembly since we wanted to avoid

any possible change to cells induced by irradiation which may interfere with the ability to conjugate particles to the cell surface. However, irradiating cells prior to the incubation with particles might be equally effective.

We considered it important to assess the stability of the assembled cell-particle hybrids against irradiation. Assembled hybrids were irradiated and the level of particle binding was compared to assembled hybrids that were not subsequently irradiated. Irradiated assemblies showed comparable levels of particle binding as detected by rhodamine fluorescence associated with particle conjugated cells and by microscopic imaging, (figures III.18 and III.19). Flow cytometric comparisons revealed a marginal decrease in mean rhodamine fluorescence in the irradiated samples (29.26) versus the non-irradiated sample (44.75), however whether this decrease is significant will need to be determined by future repeat experiments.

Applicability of the proposed assembly method to another cell line

We chose β1 integrin as a target for biotinylated antibody in the assembly of cell-particle hybrids because it is ubiquitously expressed on the cell surface of most cell types and often at high levels [102]. Although we have shown that this works for B16.F10 (melanoma cells), we wanted to investigate the ability of the same protocol to also work for other cell types. Therefore we chose a prostate cancer cell line (RM11) which also expressed high levels of β1 integrin, as demonstrated by an immunofluorescence assay (Figure III.8). We assembled a cell-particle hybrid by incubating 1 mg rhodamine-labeled streptavidin-coated particles with 5×10^5 RM11 cells for 15 minutes on ice followed by 15 minutes incubation at 37°C.

Results showed successful assembly of cell-particle hybrids with RM11 cells where test samples were associated with relative mean rhodamine levels significantly

higher than the negative control (Figure III.20). Particle binding to cells was increased significantly by increasing the particle:cell ratio by five-fold. These results are analogous to results obtained with B16.F10 cells where both rhodamine fluorescence and side scatter signals associated with cells incubated with 5 mg particles were significantly higher than that for cells incubated with 1 mg particles (Figure III.21).

Confocal microscopy images were also in agreement with flow cytometry results and revealed an increase in particle binding with increased particle:cell ratio (Figures III.22-III.23).

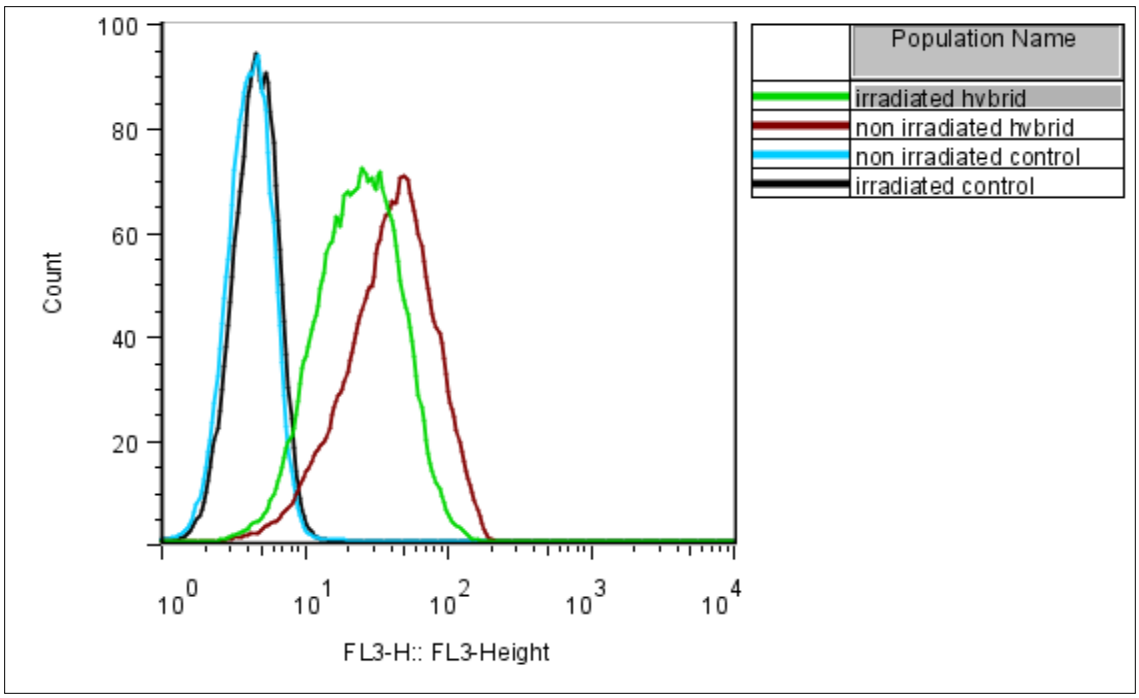

Figure III.18: Fluorescence histograms of irradiated and non-irradiated cell-particle hybrids. Rhodamine-labeled streptavidin-coated PLGA particle were incubated with biotinylated cells at 1 mg particles/ 5×10^5 cell ratios for 15 minutes on ice followed by 15 minutes incubation at 37°C. Controls involved incubating non-biotinylated cells with rhodamine-labeled streptavidin-coated PLGA particles at the same conditions as test samples. Irradiated hybrid and the associated negative control were exposed to 75Gy γ radiation prior to running all samples through the flow cytometer, n=1.

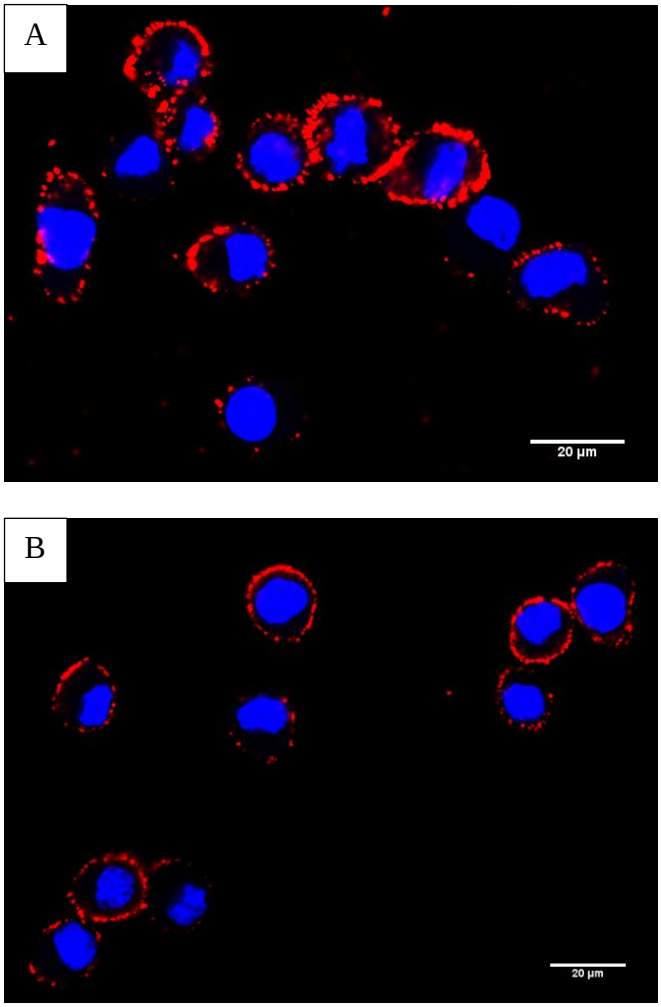

Figure III.19: Laser scanning confocal imaging of (A) irradiated and (B) non-irradiated hybrid assemblies. Rhodamine-labeled streptavidin-coated PLGA particle were incubated with biotinylated cells at 1 mg particles/5 × 10^5 cell ratios for 15 minutes on ice followed by 15 minutes incubation at 37°C. Irradiated hybrid was exposed to a γ-irradiation dose of 75 Gy. All samples were fixed in 4% paraformaldehyde and imaged using fluorescence mode at 40X. Blue = DAPI-stained cell nuclei, Red= rhodamine-labeled PLGA particles. Scale bar = 20 µm.

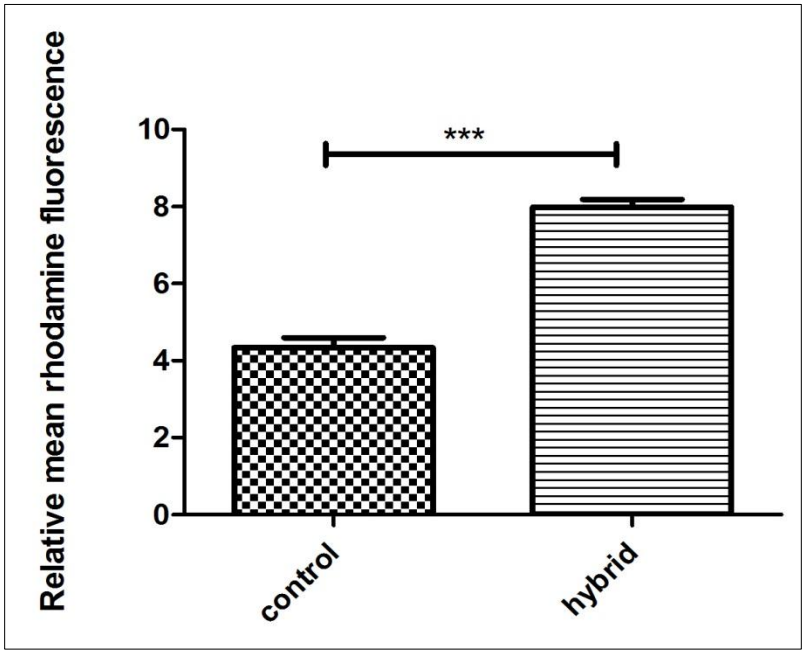

Figure III.20: Relative mean rhodamine fluorescence of cell-particle hybrid and negative control for RM11 cells. Both hybrid and controls involved the incubation of 1 mg particles with 5×10^5 cells for 15 minutes on ice followed by 15 minutes incubation at 37°C after which they were run through the flow cytometer. Legend: hybrid = rhodamine-labeled streptavidin – coated PLGA particles incubated with biotinylated cells; Control = rhodamine-labeled streptavidin – coated PLGA particles incubated with non-biotinylated cells. *** $p < 0.001$, n = 3.

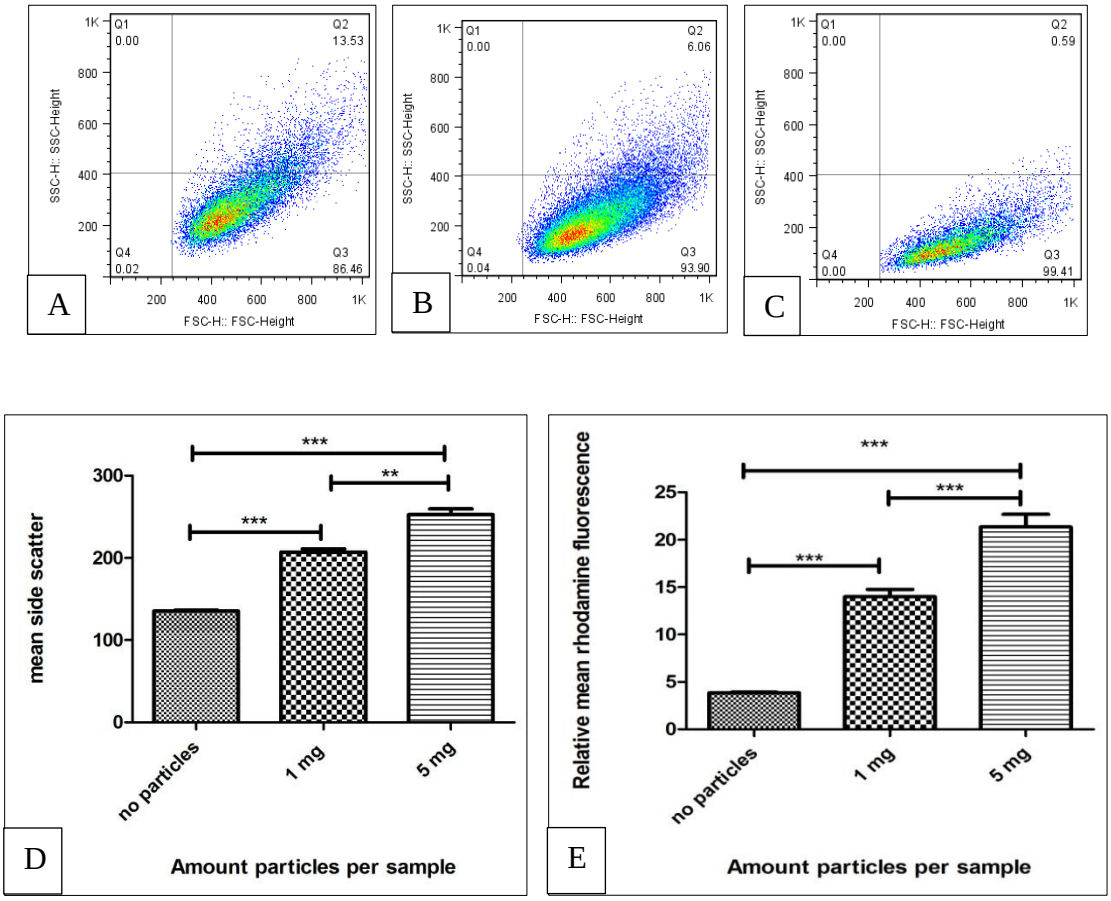

Figure III.21: Effect of particle:cell ratio on the extent of particles binding to RM11 cells. (A-C): Side scatter versus forward scatter dot plot of cell-particle hybrids assembled using varying particle: cell ratios. 5×10^5 biotinylated cell were incubated with (A): 5.0 mg, (B): 1.0 mg, (C): 0.0 mg rhodamine-labeled streptavidin-coated PLGA particle for 15 minutes on ice followed by 15 minutes incubation at 37°C prior to running through the flow cytometer. (D): Side scatter bar chart for the three treatments in (A-C), (E): relative mean rhodamine fluorescence of the three treatment groups in (A-C), for (E) data are presented as relative mean rhodamine fluorescence of test sample minus control level. n = 3, ** $p < 0.01$, *** $p < 0.001$.

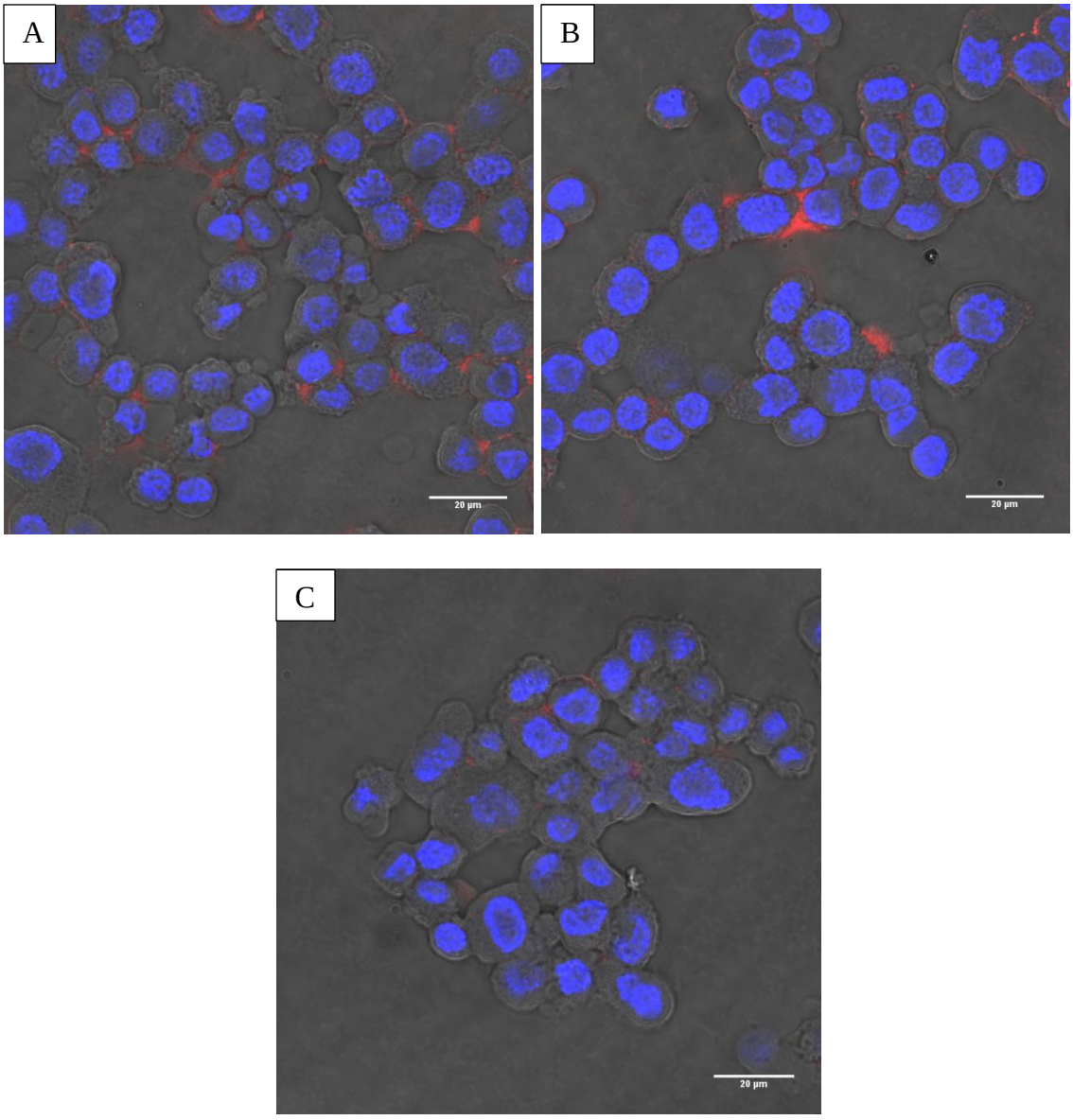

Figure III.22: Laser scanning confocal microscopy images of RM11cell-particle hybrids assembled at a ratio of 1 mg particles per 5 × 10^5 cells. Test samples: rhodamine-labeled streptavidin-coated particle were incubated with biotinylated cells for 15 minutes on ice followed by 15 minutes incubation at 37°C then samples were fixed in 4% paraformaldehyde and imaged using DIC/fluorescence mode at 63X (A,B). Control samples: non-biotinylated cells that were incubated with rhodamine-labeled streptavidin-coated particles under the same conditions as test samples (C). Blue = DAPI-stained cell nuclei, Red: rhodamine-labeled PLGA particles. Scale bar = 20 µm.

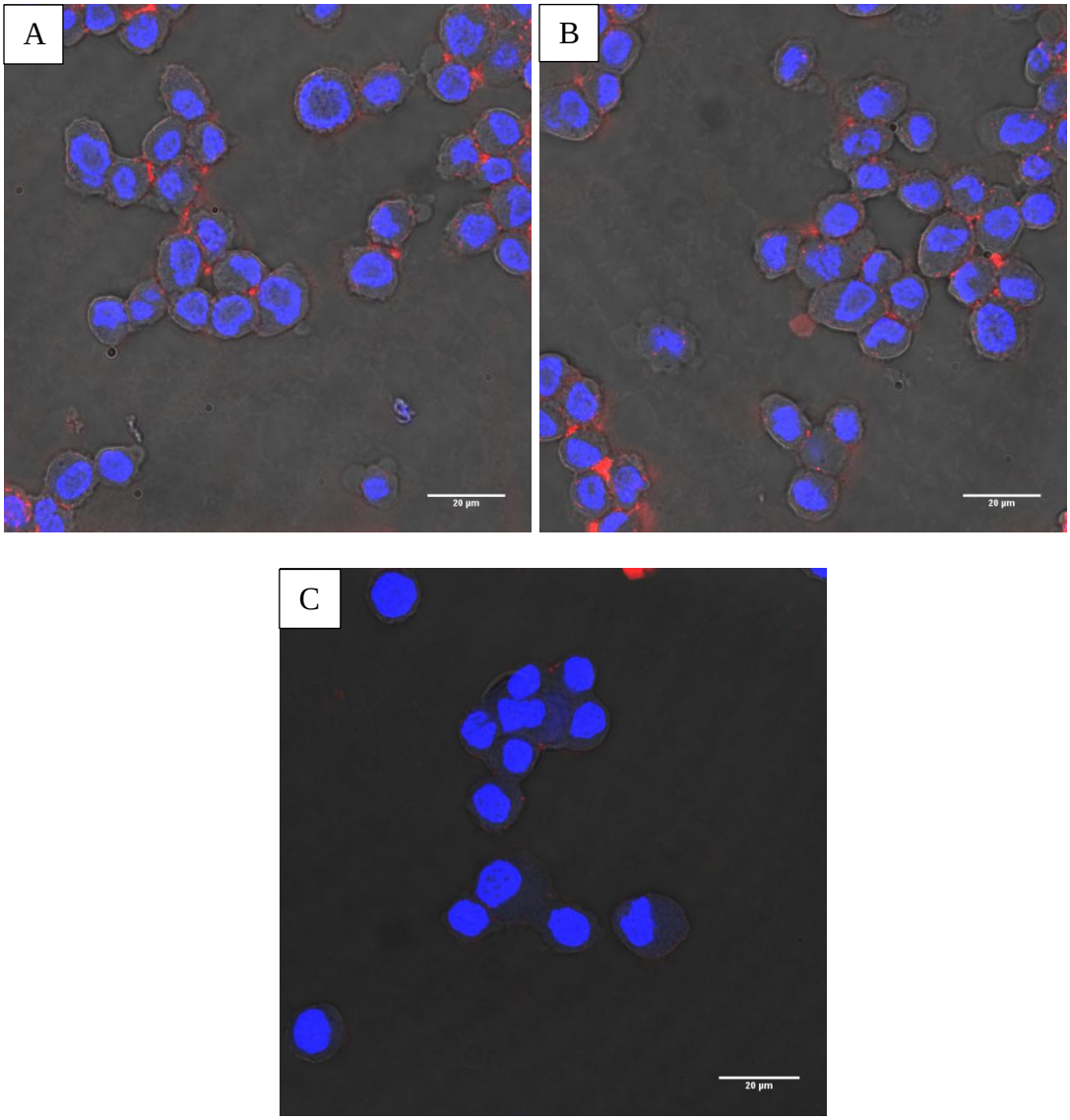

Figure III.23: Laser scanning confocal microscopy images of RM11cell-particle hybrids assembled at a ratio of 5 mg particles per 5 × 10^5 cells. Test samples: rhodamine-labeled streptavidin-coated particles were incubated with biotinylated cells for 15 minutes on ice followed by 15 minutes incubation at 37°C then samples were fixed in 4% paraformaldehyde and imaged using DIC/fluorescence mode at 63X (A,B). Control samples: non-biotinylated cells that were incubated with rhodamine-labeled streptavidin-coated particles under the same conditions as test samples (C). Blue = DAPI-stained cell nuclei, Red = rhodamine-labeled PLGA particles. Scale bar = 20 µm.

CHAPTER IV: DISCUSSION

In spite of the major achievements that have been made so far in the field of cancer therapy, cancer still represents a challenging health problem that ideally requires effective systemic treatment with minimal side effects. The prospect of using therapeutic cancer vaccines is promising, however, a lack of an effective anti-tumor immune response in clinical settings is hindering serious advancement. A key element in improving cancer vaccine efficacy is to enhance the immunostimulatory capacity of DCs. It has been shown that cancer vaccine formulations that use both CpG and GM-CSF are more efficient than either adjuvant alone [6, 89]. It also has been demonstrated that co-delivery of CpG and tumor antigen to the same DC is important in initiating strong tumor-specific immune responses [87].

In this project we developed a cell-particle hybrid system with the ultimate future goal of establishing a potential cancer vaccine system that co-delivers tumor antigens (in the form of irradiated tumor cells), and adjuvants, GM-CSF and CpG, to the same DC. The current work serves as a "proof of concept" of the feasibility of manufacturing a cell-particle hybrid system using avidin-biotin chemistry. As an initial approach, we assembled PLGA particles loaded with rhodamine rather than CpG because 1) CpG is expensive, and 2) rhodamine fluorescence can be used for the detection of successfully manufactured hybrids. We successfully managed to bind particles to the murine melanoma cell line, B16.F10. We also used the murine prostate cancer cell line (RM11) to test the possibility of applying the same method to assemble a cell-particle hybrid for other cancer cell types. Cell-particle hybrids were successfully assembled for this second cell line, also. With both cell lines the amount of particles bound per cell increased with an increasing particle:cell ratio.

Previous approaches to manufacturing cell-particle hybrids have involved nonspecific binding [57], targeting thiol residues on cell surface [93], and, to a limited

extent, avidin-biotin binding [94]. Our initial preliminary attempts to assemble cell-particle hybrids involved using electrostatic interaction. To elaborate, we coated PLGA particles with polyethylenimine (PEI) and incubated the positively charged particles (30 mV) with cells. Particles were coated with PEI using EDC/NHS chemistry and binding was assessed by the increase in rhodamine fluorescence of cells associated with PEI-coated particles. As no binding was detected, we chose to use avidin-biotin chemistry to assemble cell-particle hybrids. Avidin-biotin binding is one of the strongest types of non-covalent bond and is often used in immunological assays due to its high specificity and irreversible properties [103].

As the ultimate goal of the project is to design a cell-particle conjugate that is composed of irradiated GM-CSF-secreting tumor cells and CpG loaded particles for cancer vaccine purposes, we also investigated CpG loading of the fabricated polymeric particles and potential irradiation levels to be used. However, due to time constraints, we did not perform experiments with GM-CSF-secreting tumor cells.

Particle fabrication and modification with streptavidin

The fabricated PLGA particles showed a narrow size distribution (501.61 ± 33.64 nm) as well as having smooth surfaces (as determined by SEM), consistent with reports by other groups that used a similar fabrication method [30, 53, 104]. The negative charge (- 27 mV) of the PLGA particles was due to the terminal carboxylic acid functional groups. These functional groups are necessary for the application of EDC/NHS chemistry as a means of covalently conjugating streptavidin to the particle surface.

Particle conjugation with streptavidin via EDC/NHS chemistry was successful. The conjugated streptavidin was shown to be available for biotin binding enabling the use of streptavidin-coated particles for assembling cell-particle hybrids. This method of coating prefabricated PLGA particles with streptavidin was described in the literature and it involved similar chemistry to what we used in this project [105].

CpG loading and release

Having efficiently coated PLGA particles with streptavidin, and as the ultimate goal of the project was to manufacture cell:particle hybrids where the particles are CpG-loaded particles, we next investigated CpG loading and release profiles of uncoated PLGA particles. CpG was successfully loaded into the PLGA particles, however, total loading was lower than what was achieved previously in our lab with submicron sized particles [53] (1.63± 0.93µg/mg particles versus 2.4 ± 0.04 µg/mg particles). Next we estimated the amount of CpG remaining entrapped in streptavidin-coated CpG-loaded particles as this amount will affect how much CpG will be available in the prospective vaccine. Particle modification resulted in losing 80% of initially loaded CpG.

Two aspects should be considered regarding CpG loading. First, the amount of particulated CpG required in the vaccine dose. Second, the possible approaches toward optimizing CpG-loading into PLGA particles.

There is no literature reporting the use of particulated CpG as an adjuvant in cell-based cancer vaccines for melanoma or other cancer models. In fact, most cancer vaccines developed for melanoma that incorporated CpG involved the use of peptide antigens rather than whole cells [106]. It has been reported that the amount of CpG used in cancer vaccines involving irradiated tumor cells ranged from 10 µg of cell-conjugated CpG per vaccine dose in an E.G7 murine lymphoma model [86] to 200 µg soluble CpG per vaccine dose in a murine neuroblastoma model [6]. Between these two extremes lies a B16.F1 melanoma model that involved the incorporation of 30 µg of soluble CpG that was administered 2 and 4 days post vaccination with irradiated B16.F1 cells [107]. Our vaccine formulation, in development, will involve particulated CpG that is not only co-administered with the cells but is co-localized with the cells in the same DC. This should theoretically reduce the amount of CpG required in the vaccine formulation. However, with current CpG entrapment efficiencies of the streptavidin-coated PLGA particles (0.32 µg/mg particles after 80% loss of the original loading), approximately 30 mg of particles

will be required to provide a 10 µg CpG/ vaccine dose. This amount of particles is likely to be impractical. This argument leads us to the second aspect in considering CpG loading; the optimization of the loading efficiency so that higher amounts of CpG can be entrapped per mg of particles.

Smaller sized particles (e.g. nanoparticles/sub-micron particles) are generally associated with lower loading efficiencies and higher burst releases than larger sized particles (e.g. microparticles) due to their larger surface area to volume ratio [53]. In this project we used the double emulsion solvent evaporation technique in preparing PLGA particles that is widely adopted when a hydrophilic drug (like proteins and DNA) is to be encapsulated [108]. Many factors have been described to contribute to particle loading efficiency such as the oil phase, the emulsifier, as well as the pH and viscosity of the external aqueous phase [109, 110]. Thus, manipulating and adjusting one or more of these parameters may be one way to improve CpG loading into fabricated PLGA particles. It has been shown that for hydrophilic substances loading can be increased by using higher concentrations of PVA in the external phase [110]. The effect of increased PVA concentration on loading was attributed to the increased viscosity of the external aqueous phase that will limit outward drug diffusion, a major reason for underlying low loading efficiencies of hydrophilic drugs [111].

Antibody-mediated cell surface biotinylation

The cell surfaces of both cell lines tested (B16.F10 and RM11) were indirectly biotinylated efficiently using an integrin-specific antibody tagged with biotin. This surface-anchored biotin was available for streptavidin binding, enabling the assembly of cell-particle hybrids where particles were coated with streptavidin. Cell surface biotinylation is described in the literature for a range of purposes including cancer vaccines [74], cell therapy [112], and bioimaging [113]. A commonly used method to biotinylate cells is through the use of biotinylating reagents such as biotin hydrazide [94]

or sulfo-NHS-biotin [74, 92, 112]. This method was previously used to biotinylate cells for the purpose of subsequently binding particles [92, 94], however, using biotin hydrazide was not successful in our hands and no binding of streptavidin-coated particles to biotinylated cells could be detected. This might be due to cell line differences as the protocol we followed was reported for HEK293 cells and we used B16.F10 cells [94]. Although there was a report on biotinylating B16.F10 cells using the slightly different sulfo-NHS-biotin [74], we decided instead to look for alternatives. We therefore investigated cell surface biotinylation by employing a β1 integrin-specific antibody-tagged with biotin. β1 integrin is a type 1 transmembrane protein expressed by a variety of tumor (and normal) cells including melanoma [100]. Direct immunofluorescence confirmed the expression of relatively high levels of β1 on both B16.F10 and RM11 cell lines allowing us to proceed with using anti-β1-biotin to coat the cell surface with biotin.

Cell-particle hybrid assembly

Published reports on the assembly of cell-particle hybrids are rare and most of them lack full descriptions of methodology making reproduction of results difficult [92, 93, 114]. Our first attempt to assemble cell-particle hybrids involved incubating biotinylated cells with streptavidin-coated particles for 20 minutes on ice. However, we could not detect cell-particle binding to any measurable level where the test sample and the negative control showed similar rhodamine fluorescence levels (data not shown). While it was possible that the cell:particle mixture needed more time for efficient binding we decided to also add an incubation step at 37°C. We carried out a pilot experiment where we included variable 37°C incubation periods after 15 minutes incubation on ice and also tested whether using adherent versus suspended cells was preferable in terms of generating cell-particle hybrids (Figure III.10). The protocol for assembling cell-particle hybrids demonstrated greater efficiency when the 37°C incubation was increased from 5

to 15 minutes. This observation was further confirmed when we increased the 37°C incubation time to 30 minutes in a following experiment (Figure III.12).

There are at least two possible explanations for this observed effect of incubations at 37°C. First, at higher temperatures cells will be more metabolically active, and as a result, may be capable of, at least initiating, endocytosis. However, a study has shown that 2.8 μm sized avidin-coated particles could bind to lymphocytes efficiently in energy-independent conditions suggesting that endocytosis may not be important [115]. This is further supported in our studies by the findings, shown by SEM and confocal imaging, that the particles of the cell-particle hybrids were localized on cell surface and not internalized (Figures III.13 and III.14). Another possible contributing mechanism is the effect of temperature on targeted antigens. Although cell-particle binding takes place via avidin-biotin interaction, cells were biotinylated using antibody-linked biotin where the antibody is specific for the integrin, CD29. It is possible that cross-linking these integrins with antibodies at 37°C will result in association with the cytoskeleton resulting in integrin redistribution and gathering into patches [116]. This process of triggering antigen-antibody complex signaling (also called capping [117]) was shown to take place when antigens are cross linked via its β1 subunit [118]. We hypothesize that when particles and cells are incubated at low temperature (on ice), cell-particle binding starts taking place. When we move the system to 37°C, it could be that the gathering of receptors and their redistribution on cell surface facilitate potentially stronger binding to particles through focal adhesion-like structures (focal adhesions are regions on the cell membrane involved in cellular adhesion to extracellular matrix and they involve, among other components, structural links of surface integrins to actin cytoskeleton and external ligands [119]). Therefore when particles bind to cells at 37°C, binding will be more robust and withstand sheer effects induced by pipetting and vortex-redistribution prior to running samples through the flow cytometer. This explanation is based on the finding by others that receptor distribution and surface density affects the extent of cell-particle

binding [115]. However, at this stage we do not have proof for this hypothesis and as examining the kinetic aspects of cell-particle binding is beyond the goals of this project we did not do further investigations.

Another finding from our preliminary studies revealed that particles were bound to suspended cells more efficiently than to adherent cells. This could be attributed to the availability of more biotin for streptavidin–coated particles in case of suspended cells. To explain, when cells are biotinylated in suspension, the whole cell's surface area will be accessible for the binding of anti-β1-biotin binding thereby increasing the total biotinylated sites compared to adherent cells.

The possibility that particles were being entirely endocytosed during the optimal incubation period (15 minutes on ice followed by 15 minutes at 37°C) was eliminated by microscopic examination of the assembled cell particle hybrid. The microscopic imaging (confocal and SEM) of the cell-particle hybrid confirmed that particles are localized on cell surface. An interesting finding from the SEM images was the presence of cellular extensions in the negative control and their absence in the cell-particle assembly. This is consistent with the reported cell behavior of fibroblasts incubated with non-modified magnetic particles compared to cells incubated with cell-specific ligand modified particles [120]. The underlying causes behind these observations were not revealed and remain to be investigated.

Effect of particle:cell ratio on the extent of cell-particle binding

Another variable we looked at is the possibility of conjugating more particles per cell since the total number of particles conjugated per cell increases the amount cell-associated CpG that could potentially be delivered in the prospective vaccine. Our results showed that it is possible to increase the amount particles binding per cell (for both cell lines tested) if the particle-cell ratio is increased. This conclusion was derived based on

the increased fluorescent signal and side scatter of the test sample as particle-cell ratio increases and this was confirmed by confocal microscopy. As data shown from these experiments were generated by subtracting non-specific binding of the control, it is likely that the increased signal is due to increased avidin-biotin mediated binding. Some studies have looked at the effect of increasing particle:cell ratio on the degree of cell-particle binding. The aims of these studies were to study binding kinetics [115, 121, 122] or to examine the possibility of conjugating more particle for assembling a cell particle hybrid [57] and they involved varying linkages of cell-particle binding with one of them being close to our approach (streptavidin coated particles and antibody mediated cell biotinylation) [115]. All these studies showed that increasing particle:cell ratio increases the fraction of cells associated with particles but not the amount of particles bound per cell. However, in those studies the maximum fraction of cells binding to particles was ranging between 40-50 % with the highest particle:cell ratio employed while for this project we had a complete shift of the cell population with our initial particle:cell ratio using 1 mg particles which suggests that virtually all cells are binding to particles (Figure III.11). These results could mean that at our initial particle:cell ratio (1 mg particles:5 × 10^5 cells) we had already reached a level where all or most of cells bind to particles. Consequently further increases in particles will approach saturation of unbound receptors.

Applicability of the proposed cell-particle binding method for another tumor cell line

Having confirmed the expression of β1 integrin on RM11 cells, we then moved to assemble a cell-particle hybrid using the method described for B16.F10 cells. The flow cytometer data showed efficient cell-particle binding of streptavidin-coated particles and biotinylated cells over the negative control. The degree of binding increased with increasing particle:cell ratio. The efficient binding was demonstrated by increased rhodamine fluorescence of test samples over the negative control using flow cytometer

(Figure III.20). These results were further confirmed by laser scanning confocal imaging of the hybrid and the control (Figure III.22). These results support the hypothesis that we can apply the method suggested in this work to assemble cell-particle hybrids using β1-expressing tumor cells. Further confirmation can be provided using a third cell line that expresses β1.

Similar to results obtained for B16.F10 cells, more particles were bound per cell when cells were incubated with higher amount of particles. However, looking at laser scanning confocal images for the two cell lines we can see that more particles bound per cell in the case of B16.F10 cells for both particle:cell ratios examined. Simple qualitative assessment using confocal microscopy images is not enough to confidently draw such a conclusion and further analysis, such as counting the number particles bound per cell or measuring rhodamine fluorescence signal on the cell surface for hybrids assembled for both cell lines, will be required to confirm this conclusion. These primary findings might indicate that different cell lines will bind to particles at different levels. RM11 cells appear to express β1 integrin to a higher extent than B16.F10 cells do (analysis was done in separate work in our laboratory). Such phenomena should theoretically lead to more efficient biotinylation of cell surface and consequently more binding sites should be available for streptavidin-coated particles. However, this did not appear to be the case at least based on confocal laser scanning microscopy images. A possible explanation for limited particle binding in spite of receptor availability is the receptor distribution effect. A study was done to evaluate cell-particle binding kinetics using a similar approach to the one adopted here suggested that cell-particle binding requires receptors to be gathered or grouped on cell surface to provide receptor density sufficient to hold attached particles in place [115]. If this hypothesis is correct, it might be possible to increase cell-particle binding if we incubated the system for a longer time at 37°C so that sufficient capping of the cross-linked antigen takes place [117] and redistribution of receptors on cell surface might provide the required receptor density.

Effect of irradiation on the cell particle hybrid

The need for irradiating tumor cells prior to using them as a cancer vaccine is essential in rendering the cells immunogenic and non-proliferative [3]. As we aim to have GM-CSF secreting cells in the proposed cell-particle hybrid, it was essential that irradiation abolished the proliferative ability of the cells yet did not result in immediate cell death. In the preliminary experiments, cells treated at the three highest doses tested (35, 50, and 75 Gy) did not show any signs of proliferation in vitro, as determined by qualitative microscopy. Similarly, none of the irradiated cells led to tumor development in vivo. The effect of irradiation on GM-CSF secretion was not examined as we had not generated a GM-CSF secreting cell line at the time of these experiments. However, cancer immunotherapy studies involving the use of different irradiated GM-CSF secreting tumor cells showed that irradiation doses up to 100 Gy did not abrogate GM-CSF secretion in irradiated cells [6, 10, 58]. Further optimization of the irradiation dose might be needed depending on future in vivo cancer vaccine experiments.

The other component of the effect of irradiation is the stability of the cell-particle to irradiation. As no literature is available on irradiating cell-particle hybrids, we have chosen to irradiate cells post-assembly of cell-particle hybrids. This is because we wanted to avoid any possible changes to cells that might be induced by irradiation. As our initial attempts showed good hybrid stability, we did not investigate the possibility of irradiating cells prior to conjugating with particles, however, this alternative approach might be equally, or possibly even more, effective.

CHAPTER V: CONCLUSIONS AND FUTURE DIRECTIONS

This thesis presents the beginning stages in the manufacture of a prospective new cancer vaccine system that aims to co-deliver vaccine components (tumor cell antigens (tumor cell), and adjuvants (GM-CSF, and CpG)) to the same dendritic cells and thereby initiate strong tumor-specific cellular (CTL) immune responses. Our approach was to generate cell-particle hybrids based on avidin-biotin cross-linking where the particles were coated with streptavidin and the cells were indirectly coated with biotin using an integrin-specific biotin-labeled antibody. Cell-particle hybrids were assembled successfully using certain incubation conditions (15 minutes on ice followed by 15 minutes at 37°C incubation of suspended biotin-coated cells with streptavidin-coated PLGA particles). The addition of a 37°C incubation period showed beneficial effect toward improving the extent of cell-particle binding, yet it did not lead to complete endocytosis of conjugated particles as demonstrated by confocal and SEM images. Our preliminary studies showed good stability of the assembled cell-particle hybrid to a relatively high dose irradiation (75 Gy) as cells employed in cancer vaccines need to be irradiated both for safety and to generate tumor immunogenicity. With these results we conclude successful manufacturing of cell-particle hybrids for murine melanoma and prostate cancer tumor models.

Currently we are working on generating a GM-CSF secreting B16.F10 cell line. Once generated, it will be tested for the amount of GM-CSF secreted and the effect that irradiation has on secretion levels.

Before testing the proposed cancer vaccine for in vivo anti-tumor efficiency, we looked at the amount CpG that would be potentially delivered with current CpG loading. The results were unsatisfactory and need further investigation. CpG loading was inadequate and needed further optimization. Our primary approach toward raising the amount CpG loaded would be to adjust some of the parameters affecting loading

efficiency in the double emulsion solvent evaporation technique employed such as PVA concentration and the external phase pH. If those attempts fail to raise CpG encapsulation to an efficient level, we might consider adopting different modifications to our method for fabricating PLGA particles surface modified with streptavidin. One possibility would be to fabricate the particles using avidin-palmitate in the external aqueous phase of the double emulsion as described in the literature [123].

As mentioned earlier, the ultimate goal of the presented work is to develop a cancer vaccine system. Our results showed the feasibility of assembling cell-particle hybrids using avidin-biotin cross-linking. One of our future aims is to test the immunostimulatory efficiency of the manufactured cell-particle hybrids. Our first approach will be to test the prophylactic effect of the proposed cancer vaccine in resisting tumor challenge. This approach will also allow us to optimize levels of CpG required for efficient antitumor activity. Once the prophylactic efficiency of the vaccine is established we will move to test the therapeutic capabilities of the proposed cancer vaccine. Cancer immunotherapy, and cancer vaccine technology in particular, is a highly advancing field and the cell-particle hybrids presented here are expected to have a significant contribution to this field.

REFERENCES

1. Jemal, A., E.P. Simard, C. Dorell, A.M. Noone, L.E. Markowitz, B. Kohler, C. Eheman, M. Saraiya, P. Bandi, D. Saslow, K.A. Cronin, M. Watson, M. Schiffman, S.J. Henley, M.J. Schymura, R.N. Anderson, D. Yankey, and B.K. Edwards, Annual report to the nation on the status of cancer, 1975-2009, featuring the burden and trends in human papillomavirus (hpv)-associated cancers and hpv vaccination coverage levels. *J Natl Cancer Inst*, 2013. **105**(3): p. 175-201.

2. Yannelli, J.R. and J.M. Wroblewski, On the road to a tumor cell vaccine: 20 years of cellular immunotherapy. *Vaccine*, 2004. **23**(1): p. 97-113.

3. Charles A Janeway Jr, P.T., Mark Walport , Mark J Shlomchik. , *Immunobiology: The immune system in health and disease.* 5th edition ed. 2001, New York: Garland Science.

4. van den Engel, N.K., D. Ruttinger, M. Rusan, R. Kammerer, W. Zimmermann, R.A. Hatz, and H. Winter, Combination immunotherapy and active-specific tumor cell vaccination augments anti-cancer immunity in a mouse model of gastric cancer. *J Transl Med*, 2011. **9**: p. 140.

5. Grille, S., M. Moreno, A. Brugnini, D. Lens, and J.A. Chabalgoity, A therapeutic vaccine using salmonella-modified tumor cells combined with interleukin-2 induces enhanced antitumor immunity in b-cell lymphoma. *Leuk Res*, 2012. **37**(3): p. 341-9.

6. Sandler, A.D., H. Chihara, G. Kobayashi, X. Zhu, M.A. Miller, D.L. Scott, and A.M. Krieg, Cpg oligonucleotides enhance the tumor antigen-specific immune response of a granulocyte macrophage colony-stimulating factor-based vaccine strategy in neuroblastoma. *Cancer Res*, 2003. **63**(2): p. 394-9.

7. Dillman, R.O., C. DePriest, C. DeLeon, N.M. Barth, L.S. Schwartzberg, L.D. Beutel, P.M. Schiltz, and S.K. Nayak, Patient-specific vaccines derived from autologous tumor cell lines as active specific immunotherapy: Results of exploratory phase i/ii trials in patients with metastatic melanoma. *Cancer Biother Radiopharm*, 2007. **22**(3): p. 309-21.

8. Dillman, R.O., G.B. Fogel, A.N. Cornforth, S.R. Selvan, P.M. Schiltz, and C. DePriest, Features associated with survival in metastatic melanoma patients treated with patient-specific dendritic cell vaccines. *Cancer Biother Radiopharm*, 2011. **26**(4): p. 407-15.

9. Buchner, A., H. Pohla, G. Willimsky, B. Frankenberger, R. Frank, A. Baur-Melnyk, M. Siebels, C.G. Stief, A. Hofstetter, J. Kopp, A. Pezzutto, T. Blankenstein, R. Oberneder, and D.J. Schendel, Phase 1 trial of allogeneic gene-modified tumor cell vaccine rcc-26/cd80/il-2 in patients with metastatic renal cell carcinoma. *Hum Gene Ther*, 2010. **21**(3): p. 285-97.

10. Salgia, R., T. Lynch, A. Skarin, J. Lucca, C. Lynch, K. Jung, F.S. Hodi, M. Jaklitsch, S. Mentzer, S. Swanson, J. Lukanich, R. Bueno, J. Wain, D. Mathisen, C. Wright, P. Fidias, D. Donahue, S. Clift, S. Hardy, D. Neuberg, R. Mulligan, I. Webb, D. Sugarbaker, M. Mihm, and G. Dranoff, Vaccination with irradiated autologous tumor cells engineered to secrete granulocyte-macrophage colony-

stimulating factor augments antitumor immunity in some patients with metastatic non-small-cell lung carcinoma. *J Clin Oncol*, 2003. **21**(4): p. 624-30.

11. Le, D.T., D.M. Pardoll, and E.M. Jaffee, Cellular vaccine approaches. *Cancer J*, 2010. **16**(4): p. 304-10.

12. Schreiber, R.D., L.J. Old, and M.J. Smyth, Cancer immunoediting: Integrating immunity's roles in cancer suppression and promotion. *Science*, 2011. **331**(6024): p. 1565-1570.

13. Finn, O.J., Cancer vaccines: Between the idea and the reality. *Nat Rev Immunol*, 2003. **3**(8): p. 630-641.

14. Neller, M.A., J.A. Lopez, and C.W. Schmidt, Antigens for cancer immunotherapy. *Semin Immunol*, 2008. **20**(5): p. 286-95.

15. Chiang, C.L., F. Benencia, and G. Coukos, Whole tumor antigen vaccines. *Semin Immunol*, 2010. **22**(3): p. 132-43.

16. Buonaguro, L., A. Petrizzo, M.L. Tornesello, and F.M. Buonaguro, Translating tumor antigens into cancer vaccines. *Clin Vaccine Immunol*, 2011. **18**(1): p. 23-34.

17. de Gruijl, T.D., A.J. van den Eertwegh, H.M. Pinedo, and R.J. Scheper, Whole-cell cancer vaccination: From autologous to allogeneic tumor- and dendritic cell-based vaccines. *Cancer Immunol Immunother*, 2008. **57**(10): p. 1569-77.

18. Kenneth A. Foon, M.M.S., Activating the immune system to fight cancer. *Oncology Issues*, 2008(July/August): p. 18-24.

19. Guermonprez, P., J. Valladeau, L. Zitvogel, C. Thery, and S. Amigorena, Antigen presentation and t cell stimulation by dendritic cells. *Annu Rev Immunol*, 2002. **20**: p. 621-67.

20. Steer, H.J., R.A. Lake, A.K. Nowak, and B.W. Robinson, Harnessing the immune response to treat cancer. *Oncogene*, 2010. **29**(48): p. 6301-13.

21. Cohen, J.J., R.C. Duke, V.A. Fadok, and K.S. Sellins, Apoptosis and programmed cell death in immunity. *Annu Rev Immunol*, 1992. **10**: p. 267-93.

22. Svane, I.M., M. Boesen, and A.M. Engel, The role of cytotoxic t-lymphocytes in the prevention and immune surveillance of tumors— lessons from normal and immunodeficient mice. *Medical Oncology*, 1999. **16**(4): p. 223-238.

23. Dunn, G.P., A.T. Bruce, H. Ikeda, L.J. Old, and R.D. Schreiber, Cancer immunoediting: From immunosurveillance to tumor escape. *Nat Immunol*, 2002. **3**(11): p. 991-8.

24. Ichim, C.V., Revisiting immunosurveillance and immunostimulation: Implications for cancer immunotherapy. *J Transl Med*, 2005. **3**(1): p. 8.

25. Maher, J. and E.T. Davies, Targeting cytotoxic t lymphocytes for cancer immunotherapy. *Br J Cancer*, 2004. **91**(5): p. 817-21.

26. Lubaroff, D.M., B.R. Konety, B. Link, J. Gerstbrein, T. Madsen, M. Shannon, J. Howard, J. Paisley, D. Boeglin, T.L. Ratliff, and R.D. Williams, Phase i clinical trial of an adenovirus/prostate-specific antigen vaccine for prostate cancer: Safety and immunologic results. *Clin Cancer Res*, 2009. **15**(23): p. 7375-80.

27. McNeel, D.G., E.J. Dunphy, J.G. Davies, T.P. Frye, L.E. Johnson, M.J. Staab, D.L. Horvath, J. Straus, D. Alberti, R. Marnocha, G. Liu, J.C. Eickhoff, and G. Wilding, Safety and immunological efficacy of a DNA vaccine encoding prostatic acid phosphatase in patients with stage d0 prostate cancer. *J Clin Oncol*, 2009. **27**(25): p. 4047-54.

28. Moon, J.J., B. Huang, and D.J. Irvine, Engineering nano- and microparticles to tune immunity. *Adv Mater*, 2012. **24**(28): p. 3724-46.

29. Gupta, R. and L.A. Emens, Gm-csf-secreting vaccines for solid tumors: Moving forward. *Discov Med*, 2010. **10**(50): p. 52-60.

30. Zhang, X.Q., C.E. Dahle, N.K. Baman, N. Rich, G.J. Weiner, and A.K. Salem, Potent antigen-specific immune responses stimulated by codelivery of cpg odn and antigens in degradable microparticles. *J Immunother*, 2007. **30**(5): p. 469-78.

31. Goldstein, M.J., H.E. Kohrt, R. Houot, B. Varghese, J.T. Lin, E. Swanson, and R. Levy, Adoptive cell therapy for lymphoma with cd4 t cells depleted of cd137-expressing regulatory t cells. *Cancer Res*, 2012. **72**(5): p. 1239-47.

32. Yee, C., Adoptive t cell therapy: Addressing challenges in cancer immunotherapy. *J Transl Med*, 2005. **3**(1): p. 17.

33. Larocca, C. and J. Schlom, Viral vector-based therapeutic cancer vaccines. *Cancer J*, 2011. **17**(5): p. 359-71.

34. Schlom, J., Therapeutic cancer vaccines: Current status and moving forward. *J Natl Cancer Inst*, 2012. **104**(8): p. 599-613.

35. Higano, C.S., E.J. Small, P. Schellhammer, U. Yasothan, S. Gubernick, P. Kirkpatrick, and P.W. Kantoff, Sipuleucel-t. *Nat Rev Drug Discov*, 2010. **9**(7): p. 513-4.

36. Anderson, R.J. and J. Schneider, Plasmid DNA and viral vector-based vaccines for the treatment of cancer. *Vaccine*, 2007. **25 Suppl 2**: p. B24-34.

37. Copier, J. and A. Dalgleish, Overview of tumor cell-based vaccines. *Int Rev Immunol*, 2006. **25**(5-6): p. 297-319.

38. Sailor, M.J. and J.H. Park, Hybrid nanoparticles for detection and treatment of cancer. *Adv Mater*, 2012. **24**(28): p. 3779-802.

39. Malam, Y., E.J. Lim, and A.M. Seifalian, Current trends in the application of nanoparticles in drug delivery. *Curr Med Chem*, 2011. **18**(7): p. 1067-78.

40. Brewer, E., J. Coleman, and A. Lowman, Emerging technologies of polymeric nanoparticles in cancer drug delivery. *Journal of Nanomaterials*, 2011. **2011**.

41. Takami Akagi, M.B., Mitsuru Akashi, Biodegradable nanoparticles as vaccine adjuvant and delivery systems: Regulation of immune responses by nanoparticle-based vaccine. *Advanced polymer science* 2012. **247**: p. 31-64.

42. Hanagata, N., Structure-dependent immunostimulatory effect of cpg oligodeoxynucleotides and their delivery system. *Int J Nanomedicine*, 2012. **7**: p. 2181-95.

43. Oyewumi, M.O., A. Kumar, and Z. Cui, Nano-microparticles as immune adjuvants: Correlating particle sizes and the resultant immune responses. *Expert Rev Vaccines*, 2010. **9**(9): p. 1095-107.

44. Salem, A.K., A.D. Sandler, G.J. Weiner, X. Zhang, N.K. Baman, X. Zhu, and C.E. Dahle, 275. Immunostimulatory antigen loaded microparticles as cancer vaccines. *Mol Ther*, 2006. **13**(S1): p. S105-S105.

45. Mohsen Tafaghodi, A.S.T., Nafiseh Amiri, Plga nanospheres loaded with autoclaved *leishmania major* (alm) and cpg-odn: Preparation and in vivo characterization. *Iran J Basic Med Sci*, 2008. **11**(2): p. 112-119.

46. Xie, H., I. Gursel, B.E. Ivins, M. Singh, D.T. O'Hagan, J.B. Ulmer, and D.M. Klinman, Cpg oligodeoxynucleotides adsorbed onto polylactide-co-glycolide microparticles improve the immunogenicity and protective activity of the licensed anthrax vaccine. *Infect Immun*, 2005. **73**(2): p. 828-33.

47. Thomas, C., V. Gupta, and F. Ahsan, Particle size influences the immune response produced by hepatitis b vaccine formulated in inhalable particles. *Pharm Res*, 2010. **27**(5): p. 905-19.

48. Martinez Gomez, J.M., S. Fischer, N. Csaba, T.M. Kundig, H.P. Merkle, B. Gander, and P. Johansen, A protective allergy vaccine based on cpg- and protamine-containing plga microparticles. *Pharm Res*, 2007. **24**(10): p. 1927-35.

49. Zhang, X.Q., C.E. Dahle, G.J. Weiner, and A.K. Salem, A comparative study of the antigen-specific immune response induced by co-delivery of cpg odn and antigen using fusion molecules or biodegradable microparticles. *J Pharm Sci*, 2007. **96**(12): p. 3283-92.

50. Cruz, L.J., P.J. Tacken, R. Fokkink, B. Joosten, M.C. Stuart, F. Albericio, R. Torensma, and C.G. Figdor, Targeted plga nano- but not microparticles specifically deliver antigen to human dendritic cells via dc-sign in vitro. *J Control Release*, 2010. **144**(2): p. 118-26.

51. Dinarvand, R., N. Sepehri, S. Manoochehri, H. Rouhani, and F. Atyabi, Polylactide-co-glycolide nanoparticles for controlled delivery of anticancer agents. *Int J Nanomedicine*, 2011. **6**: p. 877-95.

52. Jeffery, H., S.S. Davis, and D.T. O'Hagan, The preparation and characterization of poly(lactide-co-glycolide) microparticles. Ii. The entrapment of a model protein using a (water-in-oil)-in-water emulsion solvent evaporation technique. *Pharm Res*, 1993. **10**(3): p. 362-8.

53. Joshi, V.B., S.M. Geary, and A.K. Salem, Biodegradable particles as vaccine delivery systems: Size matters. *AAPS J*, 2012.

54. Gutierro, I., R.M. Hernandez, M. Igartua, A.R. Gascon, and J.L. Pedraz, Size dependent immune response after subcutaneous, oral and intranasal administration of bsa loaded nanospheres. *Vaccine*, 2002. **21**(1-2): p. 67-77.

55. Kanchan, V. and A.K. Panda, Interactions of antigen-loaded polylactide particles with macrophages and their correlation with the immune response. *Biomaterials*, 2007. **28**(35): p. 5344-57.

56. Geiser, M., B. Rothen-Rutishauser, N. Kapp, S. Schurch, W. Kreyling, H. Schulz, M. Semmler, V. Im Hof, J. Heyder, and P. Gehr, Ultrafine particles cross cellular membranes by nonphagocytic mechanisms in lungs and in cultured cells. *Environ Health Perspect*, 2005. **113**(11): p. 1555-60.

57. Chambers, E. and S. Mitragotri, Long circulating nanoparticles via adhesion on red blood cells: Mechanism and extended circulation. *Exp Biol Med (Maywood)*, 2007. **232**(7): p. 958-66.

58. Dranoff, G., E. Jaffee, A. Lazenby, P. Golumbek, H. Levitsky, K. Brose, V. Jackson, H. Hamada, D. Pardoll, and R.C. Mulligan, Vaccination with irradiated tumor cells engineered to secrete murine granulocyte-macrophage colony-stimulating factor stimulates potent, specific, and long-lasting anti-tumor immunity. *Proc Natl Acad Sci U S A*, 1993. **90**(8): p. 3539-43.

59. Kanduc, D., A. Mittelman, R. Serpico, E. Sinigaglia, A.A. Sinha, C. Natale, R. Santacroce, M.G. Di Corcia, A. Lucchese, L. Dini, P. Pani, S. Santacroce, S. Simone, R. Bucci, and E. Farber, Cell death: Apoptosis versus necrosis (review). *Int J Oncol*, 2002. **21**(1): p. 165-70.

60. Obeid, M., A. Tesniere, F. Ghiringhelli, G.M. Fimia, L. Apetoh, J.L. Perfettini, M. Castedo, G. Mignot, T. Panaretakis, N. Casares, D. Metivier, N. Larochette, P. van Endert, F. Ciccosanti, M. Piacentini, L. Zitvogel, and G. Kroemer, Calreticulin exposure dictates the immunogenicity of cancer cell death. *Nat Med*, 2007. **13**(1): p. 54-61.

61. Albert, M.L., B. Sauter, and N. Bhardwaj, Dendritic cells acquire antigen from apoptotic cells and induce class i-restricted ctls. *Nature*, 1998. **392**(6671): p. 86-9.

62. Sauter, B., M.L. Albert, L. Francisco, M. Larsson, S. Somersan, and N. Bhardwaj, Consequences of cell death: Exposure to necrotic tumor cells, but not primary tissue cells or apoptotic cells, induces the maturation of immunostimulatory dendritic cells. *J Exp Med*, 2000. **191**(3): p. 423-34.

63. Brode, S. and P.A. Macary, Cross-presentation: Dendritic cells and macrophages bite off more than they can chew! *Immunology*, 2004. **112**(3): p. 345-51.

64. Multhoff, G., Heat shock proteins in immunity. *Handb Exp Pharmacol*, 2006(172): p. 279-304.

65. Zitvogel, L., O. Kepp, L. Senovilla, L. Menger, N. Chaput, and G. Kroemer, Immunogenic tumor cell death for optimal anticancer therapy: The calreticulin exposure pathway. *Clin Cancer Res*, 2010. **16**(12): p. 3100-4.

66. Clarke, C. and M.J. Smyth, Calreticulin exposure increases cancer immunogenicity. *Nat Biotech*, 2007. **25**(2): p. 192-193.

67. Obeid, M., T. Panaretakis, N. Joza, R. Tufi, A. Tesniere, P. van Endert, L. Zitvogel, and G. Kroemer, Calreticulin exposure is required for the immunogenicity of [gamma]-irradiation and uvc light-induced apoptosis. *Cell Death Differ*, 2007. **14**(10): p. 1848-1850.

68. Hoffmann, T.K., N. Meidenbauer, G. Dworacki, H. Kanaya, and T.L. Whiteside, Generation of tumor-specific t-lymphocytes by cross-priming with human dendritic cells ingesting apoptotic tumor cells. *Cancer Res*, 2000. **60**(13): p. 3542-9.

69. Dumitriu, I.E., P. Baruah, A.A. Manfredi, M.E. Bianchi, and P. Rovere-Querini, Hmgb1: Guiding immunity from within. *Trends in Immunology*, 2005. **26**(7): p. 381-387.

70. Suzuki, Y., K. Mimura, Y. Yoshimoto, M. Watanabe, Y. Ohkubo, S. Izawa, K. Murata, H. Fujii, T. Nakano, and K. Kono, Immunogenic tumor cell death induced by chemoradiotherapy in patients with esophageal squamous cell carcinoma. *Cancer Res*, 2012. **72**(16): p. 3967-76.

71. Matthew Buckwalters, P.S., Form of antigen dictates immunity: Irradiated cells vs. Whole cell lysate vaccination. *J Immunol*, 2007. **178**(S77).

72. Ravindranath, M.H., P.M. Bauer, A.A. Amiri, S.M. Miri, M.C. Kelley, R.C. Jones, and D.L. Morton, Cellular cancer vaccine induces delayed-type hypersensitivity reaction and augments antibody response to tumor-associated carbohydrate antigens (sialyl le(a), sialyl le(x), gd3 and gm2) better than soluble lysate cancer vaccine. *Anticancer Drugs*, 1997. **8**(3): p. 217-24.

73. Tarr, P., Granulocyte-macrophage colony-stimulating factor and the immune system. *Med Oncol*, 1996. **13**(3): p. 133-140.

74. Gao, J., S. Huang, M. Li, R. Luo, X. Wang, and A. Takashima, Gm-csf-surface-modified b16.F10 melanoma cell vaccine. *Vaccine*, 2006. **24**(25): p. 5265-8.

75. Kumar, H., T. Kawai, and S. Akira, Pathogen recognition by the innate immune system. *Int Rev Immunol*, 2011. **30**(1): p. 16-34.

76. Gallucci, S. and P. Matzinger, Danger signals: Sos to the immune system. *Curr Opin Immunol*, 2001. **13**(1): p. 114-119.

77. Hanna, M.G., Jr. and L.C. Peters, Immunotherapy of established micrometastases with bacillus calmette-guerin tumor cell vaccine. *Cancer Res*, 1978. **38**(1): p. 204-9.

78. Krishnamachari, Y. and A.K. Salem, Innovative strategies for co-delivering antigens and cpg oligonucleotides. *Adv Drug Deliv Rev*, 2009. **61**(3): p. 205-17.

79. Chen, H., Y. Deng, W. Tan, W. Wang, X. Yin, J. Guan, W. Wang, and L. Ruan, Impact of different adjuvants on immunogenicity of the hbv particle vaccine containing the s + pres1 fusion antigen in balb/c mice. *Chin J Biotechnol*, 2010. **26**(1): p. 74-8.

80. Lipford, G.B., T. Sparwasser, M. Bauer, S. Zimmermann, E.-S. Koch, K. Heeg, and H. Wagner, Immunostimulatory DNA: Sequence-dependent production of potentially harmful or useful cytokines. *Eur J Immunol*, 1997. **27**(12): p. 3420-3426.

81. Geary, S.M., C.D. Lemke, D.M. Lubaroff, and A.K. Salem, Tumor immunotherapy using adenovirus vaccines in combination with intratumoral doses of cpg odn. *Cancer Immunol Immunother*, 2011. **60**(9): p. 1309-17.

82. Goldstein, M.J., B. Varghese, J.D. Brody, R. Rajapaksa, H. Kohrt, D.K. Czerwinski, S. Levy, and R. Levy, A cpg-loaded tumor cell vaccine induces antitumor cd4+ t cells that are effective in adoptive therapy for large and established tumors. *Blood*, 2011. **117**(1): p. 118-27.

83. Weiner, G.J., H.M. Liu, J.E. Wooldridge, C.E. Dahle, and A.M. Krieg, Immunostimulatory oligodeoxynucleotides containing the cpg motif are effective as immune adjuvants in tumor antigen immunization. *Proc Natl Acad Sci U S A*, 1997. **94**(20): p. 10833-7.

84. Suzuki, Y., D. Wakita, K. Chamoto, Y. Narita, T. Tsuji, T. Takeshima, H. Gyobu, Y. Kawarada, S. Kondo, S. Akira, H. Katoh, H. Ikeda, and T. Nishimura,

Liposome-encapsulated cpg oligodeoxynucleotides as a potent adjuvant for inducing type 1 innate immunity. *Cancer Res*, 2004. **64**(23): p. 8754-60.

85. A K Salem, C.H.H., T W Kim, T C Wu, P C searson, K W leong, Multi-component nanorods for vaccination applications. *Nanotechnology*, 2005. **16**(4): p. 484-487.

86. Shirota, H. and D.M. Klinman, Cpg-conjugated apoptotic tumor cells elicit potent tumor-specific immunity. *Cancer Immunol Immunother*, 2011. **60**(5): p. 659-69.

87. Nierkens, S., M.H. den Brok, R.P. Sutmuller, O.M. Grauer, E. Bennink, M.E. Morgan, C.G. Figdor, T.J. Ruers, and G.J. Adema, In vivo colocalization of antigen and cpg [corrected] within dendritic cells is associated with the efficacy of cancer immunotherapy. *Cancer Res*, 2008. **68**(13): p. 5390-6.

88. Mueller, M., W. Reichardt, J. Koerner, and M. Groettrup, Coencapsulation of tumor lysate and cpg-odn in plga-microspheres enables successful immunotherapy of prostate carcinoma in tramp mice. *J Control Release*, 2012. **162**(1): p. 159-166.

89. Liu, H.M., S.E. Newbrough, S.K. Bhatia, C.E. Dahle, A.M. Krieg, and G.J. Weiner, Immunostimulatory cpg oligodeoxynucleotides enhance the immune response to vaccine strategies involving granulocyte-macrophage colony-stimulating factor. *Blood*, 1998. **92**(10): p. 3730-6.

90. Jiang, W., Y.S. KimBetty, J.T. Rutka, and C.W. ChanWarren, Nanoparticle-mediated cellular response is size-dependent. *Nat Nano*, 2008. **3**(3): p. 145-150.

91. Kirpotin, D.B., D.C. Drummond, Y. Shao, M.R. Shalaby, K. Hong, U.B. Nielsen, J.D. Marks, C.C. Benz, and J.W. Park, Antibody targeting of long-circulating lipidic nanoparticles does not increase tumor localization but does increase internalization in animal models. *Cancer Res*, 2006. **66**(13): p. 6732-40.

92. Cheng, H., C.J. Kastrup, R. Ramanathan, D.J. Siegwart, M. Ma, S.R. Bogatyrev, Q. Xu, K.A. Whitehead, R. Langer, and D.G. Anderson, Nanoparticulate cellular patches for cell-mediated tumoritropic delivery. *ACS Nano*, 2010. **4**(2): p. 625-631.

93. Stephan, M.T., J.J. Moon, S.H. Um, A. Bershteyn, and D.J. Irvine, Therapeutic cell engineering with surface-conjugated synthetic nanoparticles. *Nat Med*, 2010. **16**(9): p. 1035-1041.

94. Krishnamachari, Y., M.E. Pearce, and A.K. Salem, Self-assembly of cell–microparticle hybrids. *Advanced Materials*, 2008. **20**(5): p. 989-993.

95. Kim, R., M. Emi, and K. Tanabe, Cancer immunoediting from immune surveillance to immune escape. *Immunology*, 2007. **121**(1): p. 1-14.

96. Vesely, M.D., M.H. Kershaw, R.D. Schreiber, and M.J. Smyth, Natural innate and adaptive immunity to cancer. *Annu Rev Immunol*, 2011. **29**: p. 235-71.

97. 1-ethyl-3-(3-dimethylaminopropyl) carbodiimide hydrochloride, csid:2006116. [cited 2013 Apr 27]; Available from: http://www.chemspider.com/Chemical-Structure.2006116.html

98. N-hydroxysulfosuccinimide, csid:118082. [cited 2013 Apr 27]; Available from: http://www.chemspider.com/Chemical-Structure.118082.html

99. Biotin, csid:149962. [cited 2013 Apr 21]; Available from: http://www.chemspider.com/Chemical-Structure.149962.html

100. Feldman, L.E., K.C. Shin, R.B. Natale, and R.F. Todd, 3rd, Beta 1 integrin expression on human small cell lung cancer cells. *Cancer Res*, 1991. **51**(4): p. 1065-70.

101. Fuller-Espie, S.L., *Using flow cytometry to measure phagocytic uptake in earthworms*. Vol. 11. 2010.

102. Schmid, R.S. and E.S. Anton, Role of integrins in the development of the cerebral cortex. *Cereb Cortex*, 2003. **13**(3): p. 219-24.

103. Holmberg, A., A. Blomstergren, O. Nord, M. Lukacs, J. Lundeberg, and M. Uhlen, The biotin-streptavidin interaction can be reversibly broken using water at elevated temperatures. *Electrophoresis*, 2005. **26**(3): p. 501-10.

104. Intra, J. and A.K. Salem, Rational design, fabrication, characterization and in vitro testing of biodegradable microparticles that generate targeted and sustained transgene expression in hepg2 liver cells. *J Drug Target*, 2011. **19**(6): p. 393-408.

105. Eniola, A.O., S.D. Rodgers, and D.A. Hammer, Characterization of biodegradable drug delivery vehicles with the adhesive properties of leukocytes. *Biomaterials*, 2002. **23**(10): p. 2167-77.

106. Kochenderfer, J.N. and R.E. Gress, A comparison and critical analysis of preclinical anticancer vaccination strategies. *Exp Biol Med (Maywood)*, 2007. **232**(9): p. 1130-41.

107. Cerkovnik, P., B.J. Novakovic, V. Stegel, and S. Novakovic, Tumor vaccine composed of c-class cpg oligodeoxynucleotides and irradiated tumor cells induces long-term antitumor immunity. *BMC Immunol*, 2010. **11**: p. 45.

108. Danhier, F., E. Ansorena, J.M. Silva, R. Coco, A. Le Breton, and V. Preat, Plga-based nanoparticles: An overview of biomedical applications. *J Control Release*, 2012. **161**(2): p. 505-22.

109. Khemani, M., M. Sharon, and M. Sharon, Encapsulation of berberine in nano-sized plga synthesized by emulsification method. *ISRN Nanotechnology*, 2012. **2012**: p. 9.

110. Sahoo, S.K., J. Panyam, S. Prabha, and V. Labhasetwar, Residual polyvinyl alcohol associated with poly (d,l-lactide-co-glycolide) nanoparticles affects their physical properties and cellular uptake. *J Control Release*, 2002. **82**(1): p. 105-114.

111. Hans, M.L. and A.M. Lowman, Biodegradable nanoparticles for drug delivery and targeting. *Curr Opin Solid State Mater Sci*, 2002. **6**(4): p. 319-327.

112. Sarkar, D., P.K. Vemula, G.S. Teo, D. Spelke, R. Karnik, Y. Wee le, and J.M. Karp, Chemical engineering of mesenchymal stem cells to induce a cell rolling response. *Bioconjug Chem*, 2008. **19**(11): p. 2105-9.

113. Tannous, B.A., J. Grimm, K.F. Perry, J.W. Chen, R. Weissleder, and X.O. Breakefield, Metabolic biotinylation of cell surface receptors for in vivo imaging. *Nat Methods*, 2006. **3**(5): p. 391-6.

114. Swiston, A.J., C. Cheng, S.H. Um, D.J. Irvine, R.E. Cohen, and M.F. Rubner, Surface functionalization of living cells with multilayer patches. *Nano Letters*, 2008. **8**(12): p. 4446-4453.

115. Sarda, S., D. Pointu, F. Pincet, and N. Henry, Specific recognition of macroscopic objects by the cell surface: Evidence for a receptor density threshold revealed by micrometric particle binding characteristics. *Biophys J*, 2004. **86**(5): p. 3291-3303.

116. Mariani, G., S. Ito, R.C. Nayak, J. Baranowska-Kortylewicz, C.N. Venkateshan, A.D. Van den Abbeele, G.S. Eisenbarth, S.J. Adelstein, and A.I. Kassis, Capping and internalization of a monoclonal antibody-surface antigen complex: A possible mode of interaction of monoclonal antibodies and tumor cells. *J Nucl Biol Med*, 1991. **35**(2): p. 111-9.

117. Taylor, R.B., W.P. Duffus, M.C. Raff, and S. de Petris, Redistribution and pinocytosis of lymphocyte surface immunoglobulin molecules induced by anti-immunoglobulin antibody. *Nat New Biol*, 1971. **233**(42): p. 225-9.

118. Horvath, A.R. and S. Kellie, Regulation of integrin mobility and cytoskeletal association in normal and rsv-transformed chick embryo fibroblasts. *J Cell Sci*, 1990. **97 (Pt 2)**: p. 307-15.

119. Petit, V. and J.-P. Thiery, Focal adhesions: Structure and dynamics. *Biol Cell*, 2000. **92**(7): p. 477-494.

120. Gupta, A.K. and A.S.G. Curtis, Lactoferrin and ceruloplasmin derivatized superparamagnetic iron oxide nanoparticles for targeting cell surface receptors. *Biomaterials*, 2004. **25**(15): p. 3029-3040.

121. Peretz, V., M. Motiei, C.N. Sukenik, and R. Popovtzer, The effect of nanoparticle size on cellular binding probability. *J At Mol Opt Phys*, 2012. **2012**: p. 7.

122. Cortez, C., E. Tomaskovic-Crook, A.P. Johnston, A.M. Scott, E.C. Nice, J.K. Heath, and F. Caruso, Influence of size, surface, cell line, and kinetic properties on the specific binding of a33 antigen-targeted multilayered particles and capsules to colorectal cancer cells. *ACS Nano*, 2007. **1**(2): p. 93-102.

123. Cu, Y., C. LeMoëllic, M.J. Caplan, and W.M. Saltzman, Ligand-modified gene carriers increased uptake in target cells but reduced DNA release and transfection efficiency. *Nanomedicine*, 2010. **6**(2): p. 334-343.